INFLUENCE OF EXTREME WATER PULSES

ON GREENHOUSE GAS FLUXES FROM SOILS

by

Sandra Michele Petrakis

A thesis submitted to the Faculty of the University of Delaware in partial fulfillment of the requirements for the degree of Master of Science in Water Science and Policy

Summer 2016

INFLUENCE OF EXTREME WATER PULSES

ON GREENHOUSE GAS FLUXES FROM SOILS

by

Sandra Michele Petrakis

Approved: _____

Rodrigo Vargas, Ph.D.
Professor in charge of thesis on behalf of the Advisory Committee

Approved: _____

Shreeram P. Inamdar, Ph.D.
Director of the program of Water Science and Policy

Approved: _____

Mark W. Rieger, Ph.D.
Dean of the College of Agriculture and Natural Resources

Approved: _____

Ann L. Ardis, Ph.D.
Senior Vice Provost for Graduate and Professional Education

ACKNOWLEDGMENTS

I would like to express my most sincere gratitude towards my committee members, Rodrigo Vargas, Angelia Seyfferth, and Shreeram Inamdar, as well as JinJun Kan and Kelli Kearns from Stroud Water Research Center. I also thank William Donahoe for his support to develop an R program to calculate greenhouse gas fluxes, and Kelli Kearns, Erica Loudermilk, and Rattandeep Gill who assisted with porewater extractions and analyses. I would also like to thank our funding sources: The United States Department of Agriculture-Agriculture and Food Research Initiative (AFRI) grants 2013-02758 and 2015-67020-23585, and endowment from Stroud Water Research Center. I thank my parents, John and Beth Ann, and my brother, James, for their unwavering support and unconditional love. The perspective, wisdom, and advice you give carries me through my life, and allows me to continue to strive for, and achieve, excellence. I love you very much. I also thank my friend, Dr. Robin Kolnicki, for sharing her wisdom and always providing encouragement and inspiration. I am grateful to you and your family for opening your home, your hearts, and a wealth of knowledge to me. I also thank my many friends and colleagues around the world. Chapter two of this thesis has been submitted for review to the journal *Biogeochemistry* as of June 1st, 2016, as a manuscript titled Influence of Extreme Water Pulses on Greenhouse Gas Fluxes from Soils, and is authored by Sandra Petrakis, Angelia Seyfferth, JinJun Kan, Shreeram Inamdar, and Rodrigo Vargas.

TABLE OF CONTENTS

LIST OF TABLES vi
LIST OF FIGURES vii
ABSTRACT viii

Chapter

1 INTRODUCTION 1

2 WATER PULSE EXPERIMENT 4

2.1 Introduction to the Experiment 4
2.2 Methods 7

2.2.1 Study Site 7
2.2.2 Soil collection and analyses 8
2.2.3 Extreme water pulse experiment 9
2.2.4 Microbial community structure analysis 10
2.2.5 Soil porewater extraction and analysis 11
2.2.6 Greenhouse gas flux measurements 12
2.2.7 Data analysis 13
2.2.8 Greenhouse gas potential from soil emissions 14

2.3 Results 15

2.3.1 Soil temperature and soil moisture 15
2.3.2 Soil greenhouse gas fluxes 15
2.3.3 Relationships between soil moisture, porewater chemistry, and greenhouse gases 17
2.3.4 Total soil C, N, and microbial community dynamics 18
2.3.5 Global warming potential from soil emissions 19

2.4 Discussion 21

2.4.1 Greenhouse gas flux dynamics 21
2.4.2 Relationships among variables 24
2.4.3 C and N dynamics, and the microbial community 25
2.4.4 Global warming potential 28

2.5 Conclusions 29

TABLES 31

FIGURES 37

3 FUTURE APPLICATIONS AND POLICY IMPLICATIONS 42

REFERENCES 45

Appendix

SUPPLEMENTARY MATERIALS 52

LIST OF TABLES

Table 1 Mean values of physical and chemical properties (temperature, volumetric water content (VWC), GHGs (CO_2, CH_4, and N_2O), redox potential (Eh), pH, and porewater concentrations of Fe, S, and NO_3^-) measured during the experiment (Phases I to V) for each soil (Wetland, Creek, Forest Site 1, and Forest Site 2) Numbers in parentheses represent +/− 1 standard deviation..... 31

Table 2 Mean, minimum, and maximum values, as well as standard deviation (SD) and interquartile range (IQR) of percent change for CO_2 fluxes during the experiment (Phases I to V) for each soil 33

Table 3 Mean, minimum, and maximum values, as well as standard deviation (SD) and interquartile range (IQR) of percent change for CH_4 fluxes during the experiment (Phases I to V) for each soil. 34

Table 4 Mean, minimum, and maximum values, as well as standard deviation (SD) and interquartile range (IQR) of percent change for N_2O fluxes during the experiment (Phases I to V) for each soil. 35

Table 5 The percentages each soil (Wetland, Creek, Forest Site 1, Forest Site 2) contributed to the global warming potential (GWP) over the entire experiment for different combinations of greenhouse gases (CO_2, CH_4, and N_2O), illustrating the importance of measuring multiple greenhouse gases for 100 year and 20 year global warming potential (GWP) scenarios..... 36

LIST OF FIGURES

Figure 1 Time series of hourly data of GHGs (CO_2 CH_4, and N_2O) and volumetric water content (VWC) for Wetland (a, e, i, m) Creek (b, f, j, n), Forest Site 1 (c, g, k, o), and Forest Site 2 (d, h, l, p) soils. Vertical dashed lines represent the application of each water pulse. Roman numerals I-V denote Phases of the experiment. 37

Figure 2 Principal Component Analysis (PCA) including fluxes of GHGs (CO_2 CH_4, and N_2O), measurements of porewater chemistry (Eh, pH, Fe, S, NO_3^-), and volumetric water content (θ) for all soils during Phases II, III, IV, and V (a, b, c, and d). Soils are represented by colored points: Purple represents the Wetland, Green represents the Creek, Red represents Forest Site 1, and Blue represents Forest Site 2. 38

Figure 3 Means of percent C (a), percent N (b), and C:N ratio (c), for all soil locations before and after the re-wetting experiment. Significant differences between pre and post experimental conditions for C and N were found in the Wetland (**, $p<0.001$) and Forest Site 2 (*, $p<0.05$) soils. Forest Site 2 also showed a significant difference for pre and post experimental C:N (**, $p<0.001$) . Error bars display one standard deviation from the mean. Solid bars indicate pre-experimental values. Patterned bars indicate post-experimental values. 39

Figure 4 DGGE gel (a) showing differences in bands (arrows) for pre and post experiment conditions, labeled by soil (Wetland, Creek, Forest Site 1, and Forest Site 2), and Non-metric Multidimensional Scaling (NMDS) plots of bacterial community structure based on presence/absence of DGGE banding patterns (b). Shifts in Microbial Community Structure between the beginning (open markers) and end (closed markers) of the experiment were shown from samples of Wetland (triangles), Creek (diamonds), Forest Site 1 (squares), and Forest Site 2 (circles) soils. 40

Figure 5 Cumulative mean daily concentrations of CO_2 (a), CH_4 (b), and N_2O, given as g m^{-2}, for the Wetland (solid line), Creek (dashed line), Forest Site 1 (dotted line) and Forest Site 2 (dash-dotted line) soils. The cumulative amounts are total summations of each gas, for each soil, generated during the experiment. The cumulative amounts of each greenhouse gas, generated over the whole of the experiment, can then be converted into CO_2 equivalences ($CO_{2\text{-eq}}$), which illustrates the global warming potentials as $CO_{2\text{-eq}}$ for each soil. 41

ABSTRACT

Climate models predict increased frequency and intensity of storm events, but it is unclear how extreme precipitation events influence the dynamics of soil fluxes for multiple greenhouse gases (GHGs). Intact soil mesocosms (0-10 cm depth) from a temperate forested watershed (soils from two forested upland locations, a wetland, and a creek bank) were exposed to experimental water pulses with periods of drying, forcing soils towards extreme wet conditions under controlled temperature. We used automated measurements (hourly resolution) to monitor CO_2, CH_4, and N_2O fluxes, coupled with analyses of soil water chemistry (i.e., pH, Eh, Fe, S, NO_3^-), and microbial community structure characterized with polymerase chain reaction-denaturing gradient gel electrophoresis (PCR-DGGE). The experiment showed unexpected increases in emissions up to 244% for CO_2 (Wetland), 50988.4% for CH_4 (Creek) and 55024.3% for N_2O (Forest Site 1). The Creek soil produced the largest soil CO_2 emissions, the Wetland soil the largest CH_4 emissions, and the Forest Site 2 the largest N_2O emissions among all soils during the experiment. Using carbon dioxide equivalencies of the three GHGs, we determined that the Creek soil contributed the most to a 20-year global warming potential (GWP; 30.3%), but Forest Site 2 contributed the most to the 100-year GWP (53.7%) as a result of large N_2O emissions. These results show rapid shifts in total C, total N, microbial community structure, and porewater chemistry providing insights on the underlying mechanisms and non-linear responses of soil GHGs dynamics following experimental water pulse events.

Chapter 1

INTRODUCTION

It is more likely than not that climate change has been brought about by anthropogenic activity altering the amount of greenhouse gases (GHGs) in the earth's atmosphere, and that over some land areas it is very likely to increase in frequency, intensity, and the amount of precipitation during storms (IPCC 2013). Earth's atmosphere is approximately 0.039% CO_2, (Chapin et al. 2011) and atmospheric concentrations have increased by 40% since records began in 1750 (IPCC 2013). There is an abundance of literature documenting soil respiration of CO_2, which is one of the best studied GHGs (Schlesinger and Andrews 2000; Borken and Matzner 2009; Kim et al. 2012). Other GHGs amount to less than 0.001% of the total volume (Chapin et al. 2011). Since 1750 there has been a 150% increase in atmospheric CH_4, with the most change having occurred since 2007 (IPCC 2013). Anthropogenic contributions to increased atmospheric concentrations of CH_4 are from fossil fuels, ruminant species, and rice cultivation (Sagan and Margulis 1993), which contribute approximately 20%, 15%, and 10% of CH_4 to the atmosphere respectively (Dalal et al. 2008). CH_4 is one of the least studied GHGs, may be produced biotically, or abiotically, and its production in soils occurs under strongly reducing, anaerobic conditions through which methanogensis occurs, involves the complete mineralization of organic matter and produces CO_2 and CH_4 (Le Mer and Roger 2001; Chapin et al. 2011; Kim et al. 2012). Since 1750 there has been a 20% increase in atmospheric concentrations of N_2O

(IPCC 2013). High uncertainty and seasonal variability make it difficult to quantify N_2O emissions, though it has been reported that natural N_2O emissions from soils, oceans, and the atmosphere combined range from 5.4 to 19.6 TgN of N_2O per year (IPCC 2013). N_2O is produced in soils via nitrification, denitrification, and nitrifier denitrification, and increases have been observed following a re-wetting event over both natural ecosystems and in agricultural soils (Kim et al. 2012).

There is a need to further explore the impacts of extreme water pulse events on terrestrial ecosystems, and the mechanisms promoting or inhibiting GHG fluxes of CO_2, CH_4 and N_2O which thought they exist in the atmosphere as trace gases, contribute to increased atmospheric temperature and alterations of the hydrologic cycle associated with global warming and climate change (Chapin et al. 2011). Several studies have focused on the influence of wetting events, in the form of a pulse, on soils which have been dried, to simulate drought conditions, as climate models predict for Mediterranean and semi-arid regions (Smith et al. 2003; Muhr et al. 2008). Because gas flux responses can occur over such short temporal periods in response to a rewetting event, rapid changes in gas flux may not be captured using manual measurement techniques (Kim et al. 2012). Automated measurements at high temporal frequency are required to detect such short-term changes in soil respiration, but the instruments may be limited spatially, and though multi-spatial scale sampling is of importance, there is a trade-off between temporal and spatial sampling techniques (Savage and Davidson 2003; Kim et al. 2012). In spite of this tradeoff, high temporal frequency measurements can help to increase our understanding of the influence of biophysical conditions on biogeochemical cycling and GHG production from soils (Savage and Davidson 2003; Kim et al. 2012; Savage et al. 2014).

Soil moisture is important to biogeochemical cycling in soils, and changes in the behavior of soils would impact the types and quantities of greenhouse gas emissions, and nutrient cycling (Pilegaard et al. 2006; Cisneros-Dozal et al. 2007; Seneviratne et al. 2010; Hall et al. 2013). Both temperature and soil moisture known to be influential on the biotic processes which contribute to this soil respiration (Barron-Gafford et al. 2011). There is potential for extreme events to alter soil moisture in a manner which enhances soil contributions of GHGs (CO_2, CH_4, N_2O), and soil respiration is strongly dependent on soil moisture conditions, which if altered, could exacerbate the problem of rising global temperatures (Wang et al. 2014). That said, there are very few studies which have combined measurements of all three GHGs (Muhr et al. 2008; Kim et al. 2012; Hall et al. 2013). In the context of global warming and climate change, increased instances of extreme water pulse events could alter an ecosystem's ability to function as a carbon sink, or a sink for greenhouse gases (Seneviratne et al. 2010). However, extreme events are by their very nature rare, and as such capturing soil GHG fluxes is challenging, given the limited opportunities to do so (Vargas 2012). Thus it is important to discern how rapid, extreme changes in soil moisture might impact GHG fluxes of CO_2, CH_4 and N_2O from soils.

Chapter 2

WATER PULSE EXPERIMENT

2.1 Introduction to the Experiment

Carbon dioxide (CO_2), methane (CH_4), and nitrous oxide (N_2O) are greenhouse gases (GHGs) that contribute to global warming and feedbacks to climate change (Hartmann et al. 2013). One consequence of shifting precipitation regimes as a result of global environmental change is the increased frequency and intensity of large, powerful tropical cyclones (IPCC, 2014). As such, it is critical to understand how extreme events such as hurricanes influence ecosystem processes such as lateral transport of organic matter (Dhillon and Inamdar 2013) and vertical GHG fluxes (Vargas, 2012) around the globe. The production of these GHGs, and the potential for soils to behave as sinks or sources of these GHGs, is directly influenced by nutrient availability (Erickson and Perakis 2014), redox potential (Eh) (Dalal et al. 2008; Hall et al. 2013), temperature, and soil moisture (Davidson et al. 1998; Borken and Matzner 2009). Heavy rewetting of soils promotes reducing conditions, alters the availability of dissolved solutes and rates of C mineralization, and lowers gas diffusivity in soils (Fierer and Schimel, 2002; McNicol and Silver, 2014; Vargas, 2012). Therefore, it is important to understand the many processes involved in the production and release of GHGs from soils following rapid changes in soil moisture (Kim et al. 2012).

Recent attention has been directed towards the influence of extreme weather events on ecosystem processes (Kim et al. 2012; Sutherland et al. 2013; Frank et al. 2015). By definition, extreme weather events are rare and therefore few direct measurements of ecosystem responses to these events exist. This limits our capacity to

understand and develop prognostic capabilities for the responses of ecosystem processes. Extreme precipitation events rapidly increase soil water content and alter dynamics of GHG production in soils, with CO_2 being the most studied and well understood (Kim et al. 2012). Following rewetting, soil gas fluxes can increase by up to 9000% for CO_2, 9790% for N_2O, and smaller but uncertain responses for CH_4 (Kim et al. 2012). Many studies have addressed the addition of water to soils with either drought-stressed or dry antecedent conditions (Fierer and Schimel 2002; Smith et al. 2003; Muhr et al. 2008; Borken and Matzner 2009). Wetting of dry soils can increase microbial activity within minutes or hours, as soil organic matter is mineralized (Borken and Matzner 2009), and anaerobic conditions and decreased diffusivity may explain decreases in CO_2 fluxes under very wet conditions (Kim et al. 2012; Hall et al. 2013). Although one of the most studied terrestrial ecosystem processes is the production of CO_2 in soils (Schlesinger and Andrews 2000), there are few studies which have simultaneously measured CO_2, CH_4, and N_2O fluxes from soils with moist or very wet antecedent conditions (McNicol and Silver 2014). As such, more comprehensive understanding of the rapid responses of soils under different moisture conditions for multiple GHGs (i.e., CO_2, CH_4, and N_2O) is warranted.

Automated measurement systems can provide the temporal resolution ideal for tracking rapid changes in soil GHG emissions and responses to intense water pulses (Vargas et al. 2011; Savage et al. 2014). High temporal frequency measurements could discern the times and timescales when different biophysical mechanisms are active and relevant to GHG production in soils (Vargas et al. 2012). Because of the cost of instrumentation and availability of current technology, most studies have focused on CO_2 efflux, and few have reported continuous measurements of N_2O and CH_4 (Savage

et al., 2014). Furthermore, there is evidence supporting that the magnitude of GHG fluxes are dependent upon spatial heterogeneity and topographic location (Pacific et al. 2009; Riveros-Iregui and McGlynn 2009; Leon et al. 2014) and that a tradeoff exists between temporal and spatial sampling techniques (Savage and Davidson 2003). Thus, measuring GHG fluxes with automated measurements at high temporal frequency, while simultaneously accounting for spatial variability, is an important step in improving understanding of biogeochemical cycling, and enhancing models of GHG emissions from soils.

The development of accurate soil process-based models (Davidson et al. 2014) rather than empirical models primarily reliant on soil moisture and temperature response functions are critically needed (Aber et al. 2000; Vargas et al. 2011). The next generation of models aim to represent shorter temporal scales, such as events (i.e., pulses), while incorporating the role of a shifting microbial community and time lags of C cycling, (Vargas et al. 2011; Davidson et al. 2014). To define model architecture and parameters, we need robust data sets which include measurements of a variety of parameters within soils (e.g., pH, Eh, porewater chemistry) and to represent the rapid time scales at which biogeochemical processes occur (Bodelier and Laanbroek 2004; Xu and Luo 2012; Kim et al. 2012; Wu et al. 2015). Few process-based models simulate the production of all three major GHGs from natural soils (Zhuang et al. 2004), despite their importance for global biogeochemical cycles (Tian et al. 2016); thus, baseline information of concurrent responses of GHGs to changing weather conditions is needed across multiple ecosystems.

The overarching goal of this study was to experimentally investigate how extreme changes in water content, applied as pulses, influence GHG fluxes from different soils that occur within a forested watershed. We asked two interrelated questions: 1) What are the high temporal frequency changes in patterns and magnitude of GHG fluxes from soils in response to extreme water events? and 2) How do extreme water pulses change the soil chemistry and microbial community structure? We hypothesized that repeated extreme water pulses will force soils towards extreme wet conditions and consequently would result in a) nonlinear GHG flux responses, and b) distinct changes in soil chemistry and microbial community structure among soils. The combination of automated measurements of multiple GHGs (i.e., CO_2, N_2O, and CH_4) with analysis of porewater chemistry and microbial community structure provides novel insight into the underlying mechanisms and dynamic responses of soils to extreme weather events.

2.2 Methods

2.2.1 Study Site

The study site is a 12 ha watershed located within the Fair Hill Natural Resources Management Area (39°42' N, 75°50' W) within the Piedmont physiographic region, located in Maryland, United States. Mean annual precipitation for the study site is 1205 mm, with the highest mean monthly temperatures in July, and the lowest in January (25.7°C and -0.1 °C, respectively). In less than a decade, the Mid-Atlantic region across the United States has experienced three large Tropical Cyclone events (Nicole in 2010, Irene in 2011, and Sandy in 2012) (Dhillon and Inamdar 2013). The

forested canopy is primarily deciduous with the dominant species *Fagus grandifolia* (American beech), *Liriodendron tulipifera* (yellow poplar), and *Acer rubrum* (red maple). This watershed has an elevation range from 252 to 430 meters above sea level. Upland forest soils are classified as coarse, loamy, mixed mesic Lithic Dystrudepts in the Glenelg series. Valley bottoms contain Oxyaquatic Dystrudepts in the Baille series, but include a variety of physical and hydrological features including wetland and creek bank soils (Dhillon and Inamdar 2013).

2.2.2 Soil collection and analyses

To account for the spatial heterogeneity within the watershed, we collected soils from four locations across a topographic gradient (Table 1): an upland forested location (Forest Site 1), a downslope forested location (Forest Site 2), a wetland (Wetland), and a creek bank (Creek). Soil texture was measured using the hydrometer method for particle size analysis. Forest Site 1 soil is a sandy loam (55% sand, 26% silt, 18% clay), and Forest site 2 is a loam (45% sand, 35% silt, 20% clay), the Wetland soil is a loamy sand (83% sand 15% silt, 2% clay), and the Creek soil is sandy (96% sand, 1% silt, 3% clay). To preserve soil structure, intact soil mesocosms were collected in duplicate by inserting a 20 cm diameter PVC ring into the upper 10 cm (O and A horizons) at each one of the four locations during the early growing season (June, 2014). All soil mesocosms were immediately transported to a laboratory at the University of Delaware and adhered to Teflon planks to prevent water loss and to simulate a rise in the water table depth, allowing water accumulation in the soils.

In addition to the soil mesocosms collected for this experiment, we collected additional soil samples from the A horizon at all locations for characterization of total

C and N on pre-experimental conditions. At the conclusion of the experiment, the O horizon was removed from the soil mesocosms, and the A horizon was directly sampled from the experimental soils for comparative total C and N analyses to pre-experimental conditions. Sampled soils were analyzed using an Elementar Vario Isotope Cube (Elementar Analysensysteme GmbH Donaustraße Hanau, Germany).

2.2.3 Extreme water pulse experiment

To simulate the delivery of large amounts of water to soils as a result of extreme weather events, we conducted a water pulse experiment over a six-week period between June and July 2014. Our experimental design utilized an initial large water addition event, followed by multiple smaller events, which served to rapidly increase and maintain high soil water content throughout the experiment. The aim of these treatments was to force soils towards repeated extreme wet conditions (i.e., soil saturation) with short periods of drying to test how biogeochemical conditions are modified in a short-term timescale (i.e., days to weeks). The repeated pulses led to saturated soil conditions (Figure 1a-d), forcing soils to a different redox state, and therefore different magnitudes and patterns of GHG fluxes in the experimental soil mesocosms. We note that between pulses, the soils never became completely dry (Fig. 1a-d).

All soil mesocosms were kept under controlled laboratory conditions at room temperature (22° C) and only soil moisture was manipulated to prevent confounding effects (Davidson et al. 1998). Soil volumetric water content (VWC) and soil temperature were measured using sensors (EC-5, Decagon Devices, Pullman, WA) installed at 5 cm depth in the duplicate mesocosms of each soil. Once the intact soil mesocosms were fixed to Teflon planks (within hours of collection), we continuously

monitored soil temperature and soil moisture for 7 days prior to experimental water manipulation pulses. This 7-day period is considered pre-experimental (i.e., baseline) control conditions for each soil mesocosms, and is referred to as Phase I during the experiment. The experiment had five Phases, which included the pre-experimental Phase I, three periods where water pulses were applied (Phases II-IV), and a drying period (Phase V).

Pulses were applied with 18 MΩ·cm ultra-pure water to avoid the introduction of exogenous nutrients. Soil mesocosms were exposed to an initial large water pulse within a 5 minute period to rapidly reach saturated conditions, marking the beginning of Phase II. Thus, Phase II corresponds to an initial extreme pulse (31.8 mm) followed by a drying period of 14 days. This was followed by five smaller pulses between Phases III and IV. Phase III corresponds to the second pulse (7.9 mm) followed by a drying period of 7 days, and during Phase IV, four consecutive pulses were applied at 24-hour intervals (6.4, 3.2, 3.2, and 6.4 mm, respectively). Phase V corresponds to an 11 day drying period following the consecutive pulses of Phase IV. Previous work involving local precipitation records has reported high precipitation (i.e., >150 mm in less than 24 hours) during tropical storm Irene in 2011, which had a rainfall return period of 25 years, and moderate events correspond to <60 mm of rainfall (Dhillon and Inamdar 2013).

2.2.4 Microbial community structure analysis

To represent pre-experimental microbial conditions, we collected triplicate small soil cores (10 cm^3) from the A horizon at each sampling location in the field using modified 10 ml sterile syringes and stored them at -80° C for subsequent analysis. Post-experiment triplicate 10 cm^3 cores were also collected from the A

horizon from each experimental soil mesocosm at the end of Phase V and stored at -80° C. For analysis, these samples were thawed at room temperature, the triplicate samples for each location were homogenized, and DNA was extracted from the composites with PowerSoil DNA kits (MOBIO, Carlsbad, CA, USA). 16s rRNA genes were amplified with polymerase chain reaction (PCR), and then separated via denaturing gradient gel electrophoresis (DGGE) (Kan et al. 2006). This semi-quantitative technique can determine the presence/absence and the relative abundance of major bacterial species (Muyzer et al. 1993; Kan et al. 2006; Haugwitz et al. 2014). Using PCR-DGGE allowed us to examine bacterial population structures based on banding patterns, and determine if any changes in community structure had occurred between the beginning and the end of the experiment for each soil. Bacterial DGGE fingerprints were analyzed using GelCompar software (GelCompar II version 6.6.11, Applied Maths, Austin, TX.), which utilizes non-metric multidimensional sampling (NMDS) to compare the similarity/dissimilarity of bacterial communities among the soil samples.

2.2.5 Soil porewater extraction and analysis

Porewater from each soil was collected 11 times during the 6-week experiment between Phases II to V using Rhizon samplers (Soil Moisture Corp.), which were inserted at a 45 degree angle into the duplicate soil mesocosms at the onset of the experiment, per previous work (Seyfferth and Fendorf 2012). Porewater was collected into pre-evacuated and acid-washed vials capped under an oxygen-free atmosphere using a needle and stop-cock assembly. Eh and pH were measured immediately after porewater extraction using calibrated probes (Orion 920A+, Thermo Electron Corporation, Waltham MA; OrionStar A214 Thermo Scientific, Waltham, MA). An

additional 10 mL of porewater was taken from each soil during sampling. This was split into two 5 mL aliquots; one 5 mL aliquot was acidified with trace-metal grade HNO3 and analyzed for total Fe and S using an ICP-OES (Thermo Intrepid II Spectrometer, Thermo Fisher Scientific, Waltham MA), and the remaining 5 mL was refrigerated and later filtered through a 0.2 □m nylon membrane and used for NO3- analysis with ion chromatography (Dionex DX500, Sunnyvale, CA) with suppressed electrical conductivity. Chromatographic separation was achieved with an AG18 guard column and AS18 analytical column using a gradient elution (20.0 mM KOH for 0-15 min, 20-45 mM KOH for 15-25 min, and 20.0 for 25.5-30 min) at a flow rate of 1.0 mL min-1.

2.2.6 Greenhouse gas flux measurements

We continuously monitored soil CO_2, CH_4, and N_2O fluxes from soil mesocosms by coupling a LI-8100A (LI-COR, Lincoln Nebraska) with a Picarro G2580 analyzer (Picarro Inc, Sunnyvale California). The LI-8100A controlled a mutliplexer (LI-8150; LI-COR instruments, Lincoln Nebraska) and 20-cm autochambers (8100-104 LI-COR instruments, Lincoln Nebraska), one chamber measuring one of each of the Wetland, Creek, Forest Site 1 and Forest Site 2 intact soil mesocosms (Supplementary material 1). Each chamber was closed for a total of 6 minutes, including an observation delay of 1.5 minutes, a dead band of 30 seconds, an observation length of 3.5 minutes, and a post-purge of 30 seconds. Additionally, we measured soil temperature and soil moisture in duplicate adjacent 20 cm PVC soil mesocosms subject to the same water additions and drying.

Soil gas fluxes were calculated from the output of the Picarro G2580 analyzer using an in-house R-script following a known equation to calculate gas fluxes (Steduto

et al. 2002). Resulting gas fluxes are reported as μmol m-2 s-1 for CO_2, and nmol m-2 s-1 for CH_4 and N_2O using the following equation:

$$Soil\ GHG\ Flux = \frac{\delta c}{\delta t}\frac{V}{S}\frac{Pa}{RT} \quad \text{Equation 1}$$

where *c* is the mole fraction of a GHG in μmol mol $^{-1}$ (either CO_2, CH_4 or N_2O), t is the time of each measurement in seconds (i.e., 210 seconds), V is the total volume of the system (i.e., LI8100+LI8100M+Picarro+autochamber = 5003.6 cm^3), S is the surface area of the soil mesocosms (314.16 cm^2), Pa is the atmospheric pressure inside the chamber in kPa, R is the universal gas constant ($8.3\times10^{-3} m^3$ kPa mol^{-1} K^{-1}), and T is the air temperature (K) inside the chamber. Furthermore, we applied a quality assurance and quality control for each calculation of soil GHG fluxes. For each dc/dt in equation 1 (i.e., measurements performed during 210 seconds) we fit a linear regression for each GHG and proceeded with calculations where the slope was statistically significant ($P<0.05$) and the linear regressions had an $r^2 > 0.85$. If the P-value of the slope was >0.05, then that specific GHG flux was considered to be zero. If the P-value of the slope was <0.05 but the $r^2 < 0.85$, then the measurement was replaced as "not a number" (i.e., NaN) because uncertainty was considered to be high. Similar quality assurance and quality control protocols have been applied elsewhere (Pearson et al. 2016). Continuous time series from all chambers were processed into 1-hour intervals and filtered with a 3-hour running mean before data analysis.

2.2.7 Data analysis

We calculated the percent change in soil GHG fluxes to quantify the relative change as a result of each experimental water pulse (Kim et al 2012) (Supplementary

materials 2, 3, and 4). For this, we used the mean daily value of a GHG flux from the day before a pulse was applied as a baseline (a total of 6 baselines as 6 pulses were applied during the experiment). The relative percent change for each GHG flux was calculated using hourly data until a next pulse was applied. Hourly GHG fluxes (Fn) were divided by the corresponding baseline (Bn) and multiplied by 100 to give a percentage. We subtracted 100 to the resulting number to determine the percent increase (if a value >0) or decrease (if a value <0) from each baseline following the formula:

$$Percent\ Change = \left(\left(\frac{Fn}{Bn}\right)100\right) - 100 \qquad \text{Equation 2}$$

We first explored the linear relationships of CO_2, N_2O, CH_4, pH, Eh, Fe, S, and NO_3^- across each experimental Phase (II to V) (Supplementary materials 5, 6, 7, and 8). Then, we used principal component analysis (PCA) to analyze multivariate relationships among variables of porewater chemistry and soil GHG fluxes throughout the experiment. A two tailed *t*-test was used to test for changes in %N, %C and C/N ratio between the beginning and the end of the experiment for each soil.

2.2.8 Greenhouse gas potential from soil emissions

The cumulative radiative forcing capacity of a GHG relative to that of CO_2 (i.e., CH_4 and N_2O) is described as the global warming potential, or GWP of that gas (IPCC, 2014). We calculated these as CO_2 equivalencies ($CO_{2\text{-eq}}$) contributed by each soil for the entire experiment. For each soil we first calculated the daily sums of emissions, and converted these fluxes into g m -2 day-1 (Fig. 5). Second, the daily sums of each GHG flux were multiplied by both the upper and lower limits for (GWP)

for each respective GHG (either CO_2, N_2O, or CH_4), to obtain their $CO_{2\text{-eq}}$ (Myhre et al. 2013).We report the GWP for each GHG flux by soil as their $CO_{2\text{-eq}}$ using both 20-year and 100-year values accounting for a scenario with climate-carbon feedback (Hartmann et al. 2013), (Online Resource 9). Finally, we report the percent of total emissions each soil contributed in relation to the cumulative GHG fluxes for the entirety of the experiment as a means of quantifying the relative importance of the different GHG fluxes from soils along the experiment.

2.3 Results

2.3.1 Soil temperature and soil moisture

The mean soil temperature during the experiment was 21.9 ±0.4 °C across all soils collected from the topographic locations, illustrating negligible temperature variability under laboratory conditions (Table 1). During experimental control Phase I, mean VWC was relatively low for the Forest Site 1 (0.28 m3 m-3) and Creek soils (0.24 m3 m-3), intermediary for Forest Site 2 soil (0.34 m3 m-3) and relatively high for the Wetland soil (0.44 m3 m-3). The water pulse in Phase II and subsequent additions (Phase III-IV) substantially influenced VWC dynamics (Fig. 1a-d). Maximum VWC was observed after the final water pulse of Phase IV in the Forest Site 2 soil (0.47 m3 m-3), and the Creek showed the largest VWC variability due to high sand content (Fig. 1b).

2.3.2 Soil greenhouse gas fluxes

The highest and lowest soil CO_2 fluxes were measured from the Creek soil, which had maximum and minimum values of 4.81 µmol m-2 s-1 and 3.50 µmol m-2 s-

1, respectively (Fig. 1f). The maximum and minimum soil CO_2 fluxes for the other sites were similar, with respective maximum and minimum values of CO_2 fluxes 2.34 µmol m-2 s-1 and 0.297 µmol m-2 s-1 for Wetland, 2.62 µmol m-2 s-1and 0.514 µmol m-2 s-1 for Forest Site 1, and 2.60 µmol m-2 s-1and 0.808 µmol m-2 s-1 for Forest Site 2 (Fig. 1e,g,h).

The soil CO_2 flux dynamics showed substantial changes following water pulse additions (Supplementary material 2a-t). The greatest increase of CO_2 flux was 244%, and came from the Wetland soil during Phase V. The largest percent decrease of CO_2 flux was -195%, from the Creek soil during Phase III. Percent change of CO_2 flux in Forest Site 2 soil ranged from 58.7% to -43.5% and in Forest Site 1 soil from 129.2% to -65.7% (Table 2).

The highest soil CH_4 fluxes were measured from the Wetland soil which ranged from 192.7 nmol m-2 s-1 to -2.46 nmol m-2 s-1 (Fig. 1i), and the lowest were measured from the Creek soil which ranged from 62.6 nmol m-2 s-1 to -40.4 nmol m-2 s-1 (Fig. 1f). The maximum and minimum soil CH_4 fluxes ranged from 11.9 nmol m-2 s-1 to -2.56 nmol m-2 s-1 for the Forest Site 1 soil and 2.80 nmol m-2 s-1 to -4.25 nmol m-2 s-1 for the Forest Site 2 soil (Fig. 1g,h).

The largest changes in CH_4 flux occurred during Phase V (Table 2, Supplementary material 3) when the greatest increase in CH_4 flux of 50988.4% was observed from the Creek whereas the greatest decrease of -31832.8% was observed from the Forest Site 2 soil (Table 3). Percent change in soil CH_4 fluxes in the Wetland soil ranged from a percent increase of 276.6% to a percent decrease of -14973.7%, and in the Forest Site 1 soil from 5726.6% to -2341.9% (Table 3).

The highest soil N_2O fluxes were measured from Forest Site 2, with a maximum of 11.3 nmol m-2 s-1 followed by the Forest Site 1 with a maximum flux of 10.7 nmol m-2 s-1 (Fig. 1 p, o). The lowest overall fluxes were measured from the Wetland soil, which ranged from -0.345 nmol m-2 s-1 to 0.423 nmol m-2 s-1 (Fig. 1m). The maximum and minimum N_2O fluxes from the Creek soil were 1.98 nmol m-2 s-1 and -0.206 nmol m-2 s-1, respectively (Fig. 1n).

The largest changes to N_2O fluxes occurred during Phase II, and came from the Forest Site 1 soil which had the greatest percent increase of 55024.3% (Table 2, Supplementary material 4), and the Forest Site 2 soil with a percent decrease of -224510.8%. Percent change in the Wetland soil ranged from 1749.8% to -828.2%, and in the Creek soil from 675.1% to -174.3% (Table 4).

2.3.3 Relationships between soil moisture, porewater chemistry, and greenhouse gases

There were no linear relationships between the mean gas fluxes and mean soil moisture across any of the Phases. We did find some linear relationships between daily mean GHG fluxes and measured variables of porewater chemistry (pH, S, Fe). For example, mean soil CO2 fluxes were negatively related with porewater S in the Wetland soil (r2= 0.97, p= 0.01; Online Resource 6) and in the Creek soil (r2= 0.95, p= 0.02; Online Resource 7). Mean N2O fluxes were negatively related with porewater Fe in the Forest Site 2 soil (r2= 0.93, p= 0.02; Online Resource 8). In addition, mean N2O fluxes in the Wetland soil exhibit a positive linear relationship with mean CH4 (r2 0.93, p= 0.02; Online Resource 5) across Phases.

Due to the lack of consistency in linear relationships among variables we performed PCA for each experimental Phase to examine changes within a

multivariate space (Fig. 2). The variance explained by the PC1 varied between 56.5% and 39.6% throughout the experimental Phases (Online Resource 10), and the variables associated with each principal component changed throughout Phases II-V. In general, measurements from each soil remained individually clustered, but during Phases IV and V the Forest Site 1 and Forest Site 2 soils values began to converge. The Creek soil measurements were strongly associated with porewater pH throughout the experiment. Wetland soil measurements were associated with porewater S, and the Forest Site 2 soil measurements were associated with soil N2O fluxes across this multivariate space (Fig. 2).

The highest level of NO3- from porewater samples was found in the Creek soil during Phase IV (6.7 mg L-1), while the lowest amount of NO3- in porewater was from the Forest Site 2 soil during Phase V (0.04 mg L-1) (Table 1). Averaging each soil NO3- concentrations by Phase we found that from Phase II to Phase V, the Wetland and Creek soils began with similar levels of NO3- (0.25 mg L-1 and 0.22 mg L-1; respectively) (Table 1; Online Resource 11), which increased during Phase III and IV, and then decreased during Phase V.

2.3.4 Total soil C, N, and microbial community dynamics

Pre-experiment total soil carbon varied from a low of 1.8% in the Creek to a high of 3.4% in the Forest Site 1. At the conclusion of the experiment the Wetland soil had 9.13% C, which was the highest, and the Creek had the lowest, at 1.5 % C (Fig. 3a). Pre-experiment total soil nitrogen varied from a low of 0.12% in the Creek to 0.2% in the Forest Site 2. The Wetland soil had 0.53% N at the conclusion of the experiment, which was the highest %N of all four soils (Fig. 3b). The Creek soil had 0.1% N, which was the lowest of the four soils. (Fig. 3b). Forest Site 1 had the highest

C:N ratio for pre-experiment conditions and the Wetland had the highest C:N ratio for post-experiment conditions (Fig. 3c). Significant differences were found in pre and post-experiment % C and % N for the Wetland (t-test; $t = -11.92$, $p<0.001$; Fig 3a, t-test; $t = -18.01$, $p<0.001$; Fig. 3b), and for Forest Site 2 (t-test; $t = -7.33$, $p<0.05$; Fig. 3a, t-test; $t = -5.75$, $p<0.05$; Fig. 3b). Only Forest Site 2 showed a statistically significant difference between its pre-experiment and post-experiment C:N ratios (t-test; $t=-8.66$, $p<0.001$; Fig. 3c).

Microbial analysis of bacterial community structure was plotted with presence/absence data from DGGE fingerprints (Fig. 4a). The NMDS results displayed the differences between overall microbial community structures (Fig. 4a). The community structures among the four soils prior to the experiment were very distinct (open markers for pre-experiment, Fig. 4b), and obvious shifts in community structure were observed for all soils after the experiments (closed markers for post-experiment, Fig. 4b). Forest site 1 and Forest Site 2 soils began with dissimilar community structure, but converged at the end of the experiment. Both Creek and Wetland soils also experienced rapid community shifts, but the Wetland community structure shifted away from all of the other soils (Fig. 4).

2.3.5 Global warming potential from soil emissions

From summations of mean daily GHG fluxes we found that the Creek soil yielded the highest cumulative concentrations of CO_2, at 314 g m^{-2}, and the Wetland soil yielded the lowest cumulative concentrations of CO_2 at 160 g m^{-2} (Fig. 5a). CO_2 fluxes generated by all soils over the duration of the experiment equated to 933.5 g m^{-2}. Cumulative fluxes of CH_4 were highest from the Wetland soil, and equated to 0.57 g m^{-2} and the lowest CH_4 fluxes were from Forest Site 2 soils, equating to be -0.001 g

m^{-2} (Fig. 5b). The cumulative fluxes of CH_4 over the duration of the experiment, for all soils, equated to 1.1 g m^{-2}. Forest Site 2 soils generated the highest N_2O fluxes and sum to a total of 0.46 g m^{-2}, while the Wetland soil generated the least, equating to a total of 0.002 g m^{-2} (Fig. 5c). Cumulative fluxes of N_2O for each soil over the duration of the experiment equated to 0.72 g m^{-2}.

We examined the global warming potentials from emissions for each soil over the duration of the experiment, as $CO_{2\text{-eq}}$ (Online Resource 9). For all CO_2 emissions across measured soils, the Creek soil generated the most (33%), while the Wetland soil produced the least (16.7%; Table 5). The Forest Site 1 soil contributed 24.6% of CO_2 and Forest Site 2 soil contributed 25.05% of the total CO_2. Of the total CH_4 fluxes generated during the experiment, the Wetland contributed the most (52.36%) and the Forest Site 2 contributed the least, ultimately acting as a net sink (-1.28%; Table 5). For N_2O fluxes, the Forest Site 2 soil contributed the most (64.68%) and the Wetland soil contributed the least (0.44%; Table 5).

Adding the $CO_{2\text{-eq}}$ of CO_2, CH_4 and N_2O together changed the percentages each soil contributed to the total $CO_{2\text{-eq}}$ (Table 5). Based on a 20-year GWP scenario, the Creek had the highest percentage of total emissions (CO_2, CH_4-$CO_{2\text{-eq}}$, and N_2O-$CO_{2\text{-eq}}$; 30.3%; Table 5), whereas the Wetland soil contributed the least $CO_{2\text{-eq}}$ during the pulse experiment (16.9%; Table 5). However, based on a 100-year GWP scenario, the Forest Site 2 soil contributed the highest percentage of total emissions (53.7% in $CO_{2\text{-eq}}$), but the Wetland soil still contributed the least (2.5% in $CO_{2\text{-eq}}$; Table 5).

2.4 Discussion

2.4.1 Greenhouse gas flux dynamics

The results of this experiment provide new insights into how extreme rewetting of soils impact GHG fluxes, and provide a baseline to identify magnitudes, patterns, and biogeochemical changes. The high temporal frequency measurements (at hourly resolution) served to capture the rapid responses of GHGs to the experimental water events. Rewetting led to rapid measurable changes in Eh, microbial community structure, and GHG dynamics within each soil. We observed unprecedented shifts in GHG fluxes over 1 to 3 orders of magnitude, which to our knowledge, have not been previously reported (Kim et al 2012). These data contribute novel information about the unknown potential responses of soils to extreme weather events.

Experimental water pulses resulted in dynamic changes on soil CO2 fluxes between the beginning and end of the experiment across all soils. The differences in magnitude of CO2 fluxes from each soil draw attention to the importance of topographic position, soil properties, and hydrological patterns to the spatial variation of CO2 from soils (Pacific et al. 2009; Riveros-Iregui and McGlynn 2009; Leon et al. 2014). For example, the Wetland soil had the greatest percent increase of CO2 during the experiment (Table 2, Online Resource 2), which was 114.77% higher than the next largest increase, from Forest Site 2. The immediate suppression of CO2 fluxes corresponding to the application of each water pulse could be explained as a consequence of decreased CO2 diffusivity and increased tortuosity (Smith et al. 2003; Kim et al. 2012). Although water pulses led to overall lower CO2 fluxes at the end of the experiment, they promoted production of CH4 and N2O, which highlights the

importance of jointly measuring multiple GHGs to enhance understanding of soil GWP following extreme precipitation events.

Each soil had unique patterns and magnitudes of percent change of CH4 fluxes, supporting the importance of accounting for spatial heterogeneity and topographic position in production of GHGs (Dai et al. 2012). We expected the Wetland and Creek soils to act as a source of CH4 as is typical of freshwater wetlands (Paul et al. 2006) and inundated river floodplains (Pearson et al. 2016) and we expected to see upland forested soils as constant CH4 sinks as found in other studies of temperate forests (Smith et al. 2003; Muhr et al. 2008; Erickson and Perakis 2014). The high temporal frequency measurements captured gradual increase and decrease of CH4 from the Creek soil, and higher CH4 fluxes (nearly 50 nmol m2 s-1) from the Wetland soil at the beginning of the experiment (Fig. 1). Methane fluxes were highest for the Wetland and Creek soils during Phase III when porewater S concentrations were the lowest (Table 1), therefore providing more favorable geochemical conditions for methanogenesis (Paul et al. 2006). In Phases IV and V we observed an increase in S at both soils and a decrease in CH4 emissions. This may be attributed to an increase in NO3- which can contribute to shifts in Eh and sulfate reducing conditions (Le Mer and Roger 2001), whereby sulfate reducing bacteria may outcompete methanogenic microorganisms (Serrano-Silva et al. 2014). The steady increase in CH4 fluxes from the Forest Site 1 soil during Phase V with consistent decreases in porewater NO3- suggests favorable geochemical conditions for methanogenesis. In contrast, the increase in porewater NO3- from Forest Site 2, coupled with higher N2O emissions and higher porewater Fe concentrations, indicate biogeochemical conditions favorable for NO3- and Fe(III) reduction and unfavorable for methanogenesis. These

observations support findings from previous research where upland forest soils decreased their long-term potential as CH4 sinks under very wet conditions resulting from reduced drainage (Christiansen et al. 2012).

The magnitude of percent change in N2O fluxes for Forest Site 1 and Forest Site 2 soils are unprecedented among previous reports for rewetting of soils (Kim et al. 2012; McDaniel et al. 2014). During Phase II we observed large increases of N2O fluxes within the both Forest sites just hours after each pulse addition. This may be a consequence of available NO3- and labile dissolved organic matter as precursors to denitrification leading to rapid and high responses of N2O fluxes (Enanga et al. 2015). Denitrification may have been limited in the Creek and Wetland soils as a consequence of the low adsorption capacity of NO3- in organic soils (Paul et al. 2006). Initially, NO3- concentrations were high for both Forest Sites, but these shifted over the experiment to comparable levels from the Wetland soil in Phase II. Similar patterns of NO3- have also been observed in upland humid tropical forest soils which experienced continuous inundation (Hall et al. 2013). Although our discrete porewater samples provided snapshots of information about Eh during the experiment, we argue that continuous measurements of Eh are required to fully understand the intricacies of relationships between the GHGs production in soils and Eh. Past research shows the importance of studying the role of redox chemistry to understand the biogeochemical drivers of GHG fluxes from soils (McNicol and Silver 2014). Unfortunately, the timescales of shifts (e.g., minutes, hours, days) in Eh, coupled to other soil processes, remain unclear due to lack of automated Eh measurements in experiments and under natural conditions.

2.4.2 Relationships among variables

Although an assumption of linear responses of GHG emissions in soils to water content is commonly used (Knapp et al. 2008), overall, we did not find significant linear relationships between GHG fluxes, water content, porewater chemistry, or other GHG fluxes. This speaks to the complexity of the relationships between biophysical conditions and production of GHGs from soils that have undergone extreme rewetting events. Arguably, nonlinear models more effectively describe complex dynamics of biogeochemical processes (Manzoni and Porporato 2009). Our results emphasize the importance of these underlying biogeochemical mechanisms, and have implications for predictive capabilities, as current empirical observations and model architecture may not be suitable to predict GHG emissions from soils impacted by extreme weather events (Kim et al. 2012; Frank et al. 2015; McNicol and Silver 2015).

Using a multivariate approach identified shifts on the relative importance of biogeochemical variables across the different soil types over the Phases of the experiment (Fig. 2). Certain vectors in our PCA were consistently associated with specific soil types. For example, the Wetland soil was associated with S; this could be explained by the potential presence of sulfate reducing bacteria (Pester et al. 2012; Serrano-Silva et al. 2014). Forests soils were consistently associated with N_2O, likely as a result of their sensitivity to soil conditions which would promote denitrification (Pilegaard et al. 2006; Chapin et al. 2011) and therefore the higher levels of N_2O fluxes from these soils. The Creek soils were consistently associated with the highest porewater pH values, which also increased over the duration of the experiment. An increase in pH is associated with decreasing electron activity (i.e., lower Eh) (Essington 2004; Grybos et al. 2009) and Fe(II) appears at a pH of 6.5 if electron

activity is very low (Essington 2004), potentially explaining why observed porewater Fe and pH vectors were associated with the Creek soil in Phase III (Fig. 2b).

At the conclusion of the experiment we observed convergence in multivariate space of the two Forest Site soils with a strong association to porewater Fe and N_2O (Fig. 2d). Higher values of Fe and pH have been found in acidic, waterlogged soils associated with reduction of NO_3^- and Fe (Grybos et al. 2009). The Wetland soil remained associated to S and Eh suggesting that extreme water pulses have little effect on its biogeochemistry, as these soils are typically associated with inundated anoxic conditions (Zhuang et al. 2004). However, drying of wetland soils greatly impacts their biogeochemistry by allowing for rapid turnover of labile organic matter as the microbial community shifts to aerobic metabolism (Davidson et al. 2014; McNicol and Silver 2015). Unlike the Wetland soil, the Creek soil substantially changed its associations in the multivariate space, indicative of sensitivity of its biogeochemistry in response to the water pulses. These soils are analogous to floodplains that may undergo substantial rewetting and drying events depending on runoff and water level, therefore shifting their potential to become sink or source of GHGs along the year (Pearson et al. 2016).

2.4.3 C and N dynamics, and the microbial community

Examining shifts of the microbial community structure and C and N dynamics provided an additional perspective on the impact of extreme water pulses on soil GHG fluxes. Previous studies observed that microbial community structure is sensitive to water stress (Davidson et al. 1998; Schimel et al. 2007) and changes in pH (Fierer and Jackson 1998) which we observed from our porewater samples (Table 1). Each soil began with a distinct microbial community structure, but with extreme wet conditions

brought on by water pulse applications, and consequent periods of drying, the microbial community structure shifted in different directions (in the multivariate space of dimensions 1 and 2; Fig. 4b).

Long term effects on soil respiration, such as a decrease in CO_2 fluxes which we observed across all soils, may be a result of decreased metabolic capacity of the microbial community under suboxic and anoxic conditions and can be instigated by a single rewetting event, which previous research has shown can lead to a decrease in respiration by as much as 25% (Schimel et al. 2007). Fluxes of CH_4 observed from the Forest Site 1 soil at the end of the experiment (Fig. 1k) indicate an active community of methanogens. Moreover, the response of N_2O fluxes from the Creek, Forest Site 1, and Forest Site 2 soils to water pulses (Fig. 1n, o, p) suggests population structure or activity changes in nitrogen transforming microorganisms (i.e., nitrifiers and denitrifiers). We did not excise the DGGE bands for sequencing, therefore we do not identify bacterial species present on DGGE gel. DGGE is a quick fingerprinting approach, which provides a "snapshot" on the dominant bacteria from the community (Gelsomino et al., 1999; Kan et al., 2006). Most of the minor or rare species will be skipped from the fingerprinting approaches such as DGGE. Determining the detailed bacterial community changes would require (1) appropriate primers targeting at specific groups of bacteria (e.g., methanogens, methanotrophs, nitrifiers, denitrifiers etc.) or (2) more detailed bacterial community characterization approaches including high throughput sequencing (Jenkins and Gibson 2002). Future studies targeting methanogenic/methanotrophic and nitrifying/denitrifying groups of microorganisms could enhance understanding of patterns of CH_4 and N_2O seen from soils in response

to repeated global climate changes such as extreme precipitation events and consequently longer flooding periods.

Differences between total C and N values between the beginning and end of the experiment (Fig. 3a,b) indicate rapid changes in organic matter decomposition (from the O-horizon) influenced by the additions of water during the experiment. One contributing factor may be the transport of solutes from cells, and cell lysis, which are both linked to rapid increases of soil moisture and enhanced decomposition, and release nutrients into the soil (Fierer and Schimel 2003; Cisneros-Dozal et al. 2007). In temperate watersheds, the accumulation of C tends to occur in near-stream zones, which may be a limiting factor to denitrifying species (Cirmo and McDonnell 1997) and could relate to limited fluxes of N_2O from the Wetland and Creek soils. We also observed macroinvertebrates (earthworms) in the Forest Site 1 and Forest Site 2 soils during collection of A horizon soils for post experimental analysis, which are known to stimulate N cycling and decomposition, increase infiltration through creation of macropores, and enhance CH_4 oxidation (Levia et al. 2011; Serrano-Silva et al. 2014). Furthermore, additions of C and N release NO and NO_2, which are both toxic to methanogenic archaea, and might relate to the inhibited CH^4 fluxes we observed within the Wetland soil (Kim et al. 2015). While no outside sources of C or N were added to our soil mesocosms (O and A horizons) during our experiment, the observed increases in percent C and percent N from our Wetland, Forest Site 1, and Forest Site 2 Soils (Fig. 3), may be due to transfer of C and N from the decomposition of leaf litter (O horizon) to the A-horizon during the experiment (Borken and Matzner 2009; Chapin et al. 2011), since only the A horizon was sampled in both pre and post experiments. It is known that pulses of water bring dissolved organic carbon sources

from leaf litter into soils, and break aggregates, releasing different pools (e.g., labile, recalcitrant) of C into deeper horizons (Xu and Luo 2012). The decrease in VWC measured in the Wetland soil during Phase V (Fig. 1a) may have allowed for an increase in aerobic metabolism, and therefore higher decomposition of labile organic matter in the O-horizon that could have transferred C into the A-horizon.

2.4.4 Global warming potential

We used the GWP to bring attention to how extreme rewetting events might influence the temporal dynamics of multiple GHGs, how distinct soils might contribute to global warming, and the role of spatial heterogeneity of soils to understand GHG emissions from soils across watersheds and complex terrain. The summation of the mean daily GHG fluxes was important because it allowed us to calculate the GWP in $CO_{2\text{-eq}}$ for each gas from each soil. The dataset generated from high temporal frequency measurements allowed us to accomplish this. Although the cumulative amounts of CH_4 and N_2O were smaller than those of CO_2 (Fig. 5), the different contributions of each soil as influenced by repeated water pulses, and the higher GWPs of these GHGs, reinforces the need to explore the potential for changes under extreme hydrologic conditions, while accounting for spatial heterogeneity of soils within ecosystems (Kim et al. 2012).

The Creek soil had the most CO_2 efflux, the Wetland contributed the most CH_4 efflux, and Forest Site 2 contributed the most N_2O efflux. With this information we examined the GWP for each soil using the 20-year and 100-year values (Hartmann et al. 2013). The Wetland soil was responsible for the lowest GWP in comparison to other soils because although CH_4 has a higher radiative forcing capacity, it is relatively short lived in the atmosphere (Smith et al. 2003). Using 20-year GWP

values, we found the Creek contributed the most to the total $CO_{2\text{-eq}}$, as this soil had the largest fluxes of CO_2, and some CH_4 and N_2O. In contrast, when using the 100-year GWP values, we found that the Forest Site 2 Soil had the largest impact as a result of increases of N_2O emissions, and highlights the important role of N_2O in temperate forested ecosystems (Enanga et al. 2015). Calculating the cumulative GWP of multiple GHGs from soils was a useful way to visualize the impacts of extreme water pulses on each of our soils, and these results emphasize the importance of automated measurements to capture rapid changes in soil GHGs emissions.

2.5 Conclusions

High temporal frequency measurements of CO_2, N_2O and CH_4 provided the ability to explore rapid responses of GHG flux to experimental water addition. We observed unprecedented changes in magnitude of GHG fluxes, showing the potential for change in soil GHG flux dynamics. The rapid shifts from the beginning to the end of the experiment for C, N and microbial community structures indicate that extreme water pulses can substantially impact C and N dynamics, and microbial community composition at short temporal scales (i.e., < 2 months). Our results support the need for models to account for nonlinear relationship between GHG fluxes and driving variables, as well as spatial heterogeneity across landscapes and in complex terrain, and incorporate the sensitivity of biogeochemical mechanisms for production and consumption of GHGs from soils. Combining automated measurements of CO_2, CH_4, and N_2O across different soils provided a new perspective of the full global warming potential by GHG emissions from soils following extreme rewetting events. To better understand the sensitivity of GHG fluxes to redox, it may be beneficial to incorporate automated measurements of Eh in conjunction with automated measurements of all 3

GHGs. Finally, we argue that because extreme events are uncommon, the opportunities to capture ecosystem responses are limited; therefore experimental manipulation is an alternative method by which we can advance our understanding of responses to uncommon biophysical conditions.

TABLES

Table 1 Mean values of physical and chemical properties (temperature, volumetric water content (VWC), GHGs (CO_2, CH_4, and N_2O), redox potential (Eh), pH, and porewater concentrations of Fe, S, and NO_3^-) measured during the experiment (Phases I to V) for each soil (Wetland, Creek, Forest Site 1, and Forest Site 2) Numbers in parentheses represent +/− 1 standard deviation.

Location	Wetland					Creek					Forest Site 1					Forest Site 2				
Mean Values by Phase	I	II	III	IV	V	I	II	III	IV	V	I	II	III	IV	V	I	II	III	IV	V
Temperature (°C)	21.6 (0.2)	21.8 (0.2)	21.8 (0.3)	21.9 (0.2)	21.7 (0.2)	22.2 (0.4)	21.6 (0.5)	21.4 (0.3)	21.6 (0.2)	21.7 (0.5)	22.2 (0.2)	22.1 (0.2)	22.1 (0.3)	22.2 (0.2)	21.9 (0.2)	22.2 (0.3)	22.4 (0.2)	22.3 (0.2)	22.3 (0.2)	22.0 (0.2)
VWC (m^{-3} m^{-3})	0.4 (0.01)	0.5 (0.01)	0.5 (0.01)	0.5 (0.01)	0.4 (0.01)	0.2 (0.00)	0.4 (0.05)	0.4 (0.05)	0.3 (0.03)	0.3 (0.05)	0.3 (0.03)	0.4 (0.04)	0.4 (0.02)	0.4 (0.01)	0.4 (0.01)	0.3 (0.01)	0.4 (0.05)	0.4 (0.01)	0.5 (0.01)	0.5 (0.01)

Table 1 continued

CO_2 (μmol m^{-2} s^{-1})	1.6 (0.4)	0.7 (0.4)	1.0 (0.4)	0.8 (0.4)	0.9 (0.4)	4.4 (0.4)	1.2 (1.2)	1.8 (0.8)	1.7 (0.5)	1.7 (0.4)	2.3 (0.1)	1.1 (0.4)	1.2 (0.4)	1.3 (0.3)	1.5 (0.5)	2.2 (0.1)	1.5 (0.2)	1.3 (0.2)	1.3 (0.2)	1.3 (0.2)
CH_4 (nmol m^{-2} s^{-1})	18.6 (8.7)	10.9 (15.6)	17.8 (34.7)	0.0 (0.1)	0.9 (1.3)	-0.1 (0.1)	1.7 (2.7)	19.5 (14.9)	0.6 (1.0)	3.7 (4.4)	-1.2 (0.2)	0.1 (1.4)	0.0 (0.4)	0.0 (0.4)	3.5 (3.8)	-1.6 (0.2)	-0.3 (0.9)	-0.1 (0.5)	0.0 (0.1)	0.0 (0.3)
N_2O (nmol m^{-2} s^{-1})	0.1 (0.1)	0.1 (0.1)	0.1 (0.1)	-0.1 (0.1)	-0.1 (0.1)	0.4 (0.2)	0.1 (0.2)	0.5 (0.5)	0.8 (0.6)	0.1 (0.1)	0.1 (0.1)	2.8 (2.7)	0.8 (0.3)	1.2 (0.3)	1.1 (0.8)	0.0 (0.1)	3.8 (3.1)	3.7 (2.2)	5.9 (2.7)	1.4 (2.0)
Eh (RMV)	N/A	229.7 (N/A)	221.5 (40.0)	174.9 (85.2)	267.4 (42.3)	N/A	164.5 (N/A)	170.8 (36.2)	72.4 (160.0)	218.8 (55.9)	N/A	257.4 (N/A)	239.8 (20.2)	85.4 (181.1)	244.7 (42.1)	N/A	554.9 (N/A)	233.8 (33.4)	94.3 (158.4)	227.2 (24.8)
pH	N/A	5.2 (N/A)	5.2 (0.2)	4.8 (0.9)	5.0 (0.2)	N/A	6.1 (N/A)	6.5 (0.1)	6.3 (1.1)	6.6 (0.1)	N/A	4.9 (N/A)	5.3 (0.3)	5.3 (0.8)	5.3 (0.1)	N/A	4.4 (N/A)	5.4 (0.1)	5.6 (0.0)	5.7 (0.1)
Fe (mg L^{-1})	N/A	21.8 (N/A)	0.9 (1.1)	0.2 (0.1)	1.4 (2.2)	N/A	0.2 (N/A)	13.6 (6.3)	3.5 (0.3)	2.3 (1.2)	N/A	0.5 (N/A)	9.5 (2.6)	8.4 (2.3)	31.6 (20.8)	N/A	1.1 (N/A)	15.3 (4.2)	8.9 (3.1)	31.3 (4.1)
S (mg L^{-1})	N/A	34.9 (N/A)	16.7 (7.9)	27.8 (1.3)	20.3 (8.1)	N/A	10.0 (N/A)	2.9 (0.7)	4.2 (0.4)	5.4 (1.0)	N/A	6.6 (N/A)	5.5 (0.2)	5.2 (0.1)	8.5 (3.1)	N/A	17.9 (N/A)	6.3 (1.0)	6.4 (0.7)	9.7 (4.5)
NO_3^- (mg L^{-1})	N/A	1.3 (N/A)	1.7 (0.6)	2.9 (0.0)	3.6 (2.8)	N/A	1.2 (N/A)	7.8 (4.2)	30.2 (2.6)	10.3 (5.2)	N/A	12.2 (N/A)	9.2 (11.2)	6.7 (3.4)	3.9 (2.6)	N/A	23.4 (N/A)	1.5 (0.3)	1.5 (0.1)	3.5 (2.2)

Table 2 Mean, minimum, and maximum values, as well as standard deviation (SD) and interquartile range (IQR) of percent change for CO_2 fluxes during the experiment (Phases I to V) for each soil.

		% Change CO_2				
	Soil	Mean	Minimum	Maximum	SD	IQR
All Phases	Wetland	25.5	-81.1	244.0	90.4	325.1
	Creek	1.3	-195.8	98.6	56.7	294.5
	Forest Site 1	10.2	-65.7	129.2	53.1	194.9
	Forest Site 2	1.0	-43.5	58.7	25.1	102.2
Phase I	Wetland	27.2	-1.3	80.3	29.7	81.6
	Creek	12.6	-10.5	21.7	9.4	32.2
	Forest Site 1	2.5	-7.5	13.4	5.1	20.9
	Forest Site 2	-6.5	-14.6	7.6	5.2	22.2
Phase II	Wetland	-67.4	-81.1	4.0	18.6	85.1
	Creek	-74.0	-97.0	-3.7	25.0	93.3
	Forest Site 1	-53.3	-65.7	-2.1	15.6	63.6
	Forest Site 2	-26.3	-38.1	23.8	17.5	61.9
Phase III	Wetland	10.0	-58.9	83.5	48.5	142.4
	Creek	-7.4	-195.8	34.3	41.4	230.1
	Forest Site 1	11.0	-47.8	70.5	39.9	118.2
	Forest Site 2	-1.3	-23.4	22.5	13.0	45.9
Phase IV	Wetland	-51.1	-79.5	4.2	22.3	83.7
	Creek	-33.9	-86.0	-3.3	18.7	82.6
	Forest Site 1	-30.1	-63.6	0.7	16.1	64.2
	Forest Site 2	-16.7	-43.5	7.1	13.7	50.7
Phase V	Wetland	111.5	-4.0	244.0	93.9	248.0
	Creek	56.1	-48.2	98.6	38.1	146.8
	Forest Site 1	56.3	-20.9	129.2	47.8	150.1
	Forest Site 2	24.8	-6.8	58.7	22.8	65.5

Table 3 Mean, minimum, and maximum values, as well as standard deviation (SD) and interquartile range (IQR) of percent change for CH_4 fluxes during the experiment (Phases I to V) for each soil.

		% Change CH_4				
	Soil	Mean	Minimum	Maximum	SD	IQR
All Phases	Wetland	-826.0	-14973.7	276.6	2226.5	15250.3
	Creek	994.6	-5876.9	50988.4	3946.8	56865.4
	Forest Site 1	443.8	-2341.9	5726.6	1332.3	8068.5
	Forest Site 2	-320.8	-31832.8	2304.0	1980.8	34136.8
Phase I	Wetland	45.0	-17.8	265.2	70.6	283.0
	Creek	56.1	-86.5	402.4	90.1	489.0
	Forest Site 1	33.4	-3.9	78.4	26.7	82.3
	Forest Site 2	15.7	-12.2	38.6	14.5	50.8
Phase II	Wetland	-23.4	-99.8	266.5	105.5	366.3
	Creek	-1085.6	-5617.5	1604.2	1560.5	7221.7
	Forest Site 1	-98.5	-460.2	76.2	82.4	536.5
	Forest Site 2	-93.8	-478.6	66.5	76.6	545.2
Phase III	Wetland	-54.3	-103.9	276.6	80.6	380.5
	Creek	54.6	-5876.9	6735.4	1155.1	12612.4
	Forest Site 1	-99.8	-221.1	281.5	47.5	502.5
	Forest Site 2	-83.8	-186.4	455.3	62.9	641.7
Phase IV	Wetland	-104.7	-266.8	5.2	40.7	272.0
	Creek	-91.2	-102.0	-39.9	14.6	62.1
	Forest Site 1	-268.6	-2341.9	384.0	481.8	2725.9
	Forest Site 2	-767.5	-7467.7	2304.0	1493.7	9771.7
Phase V	Wetland	-2503.9	-14973.7	-20.0	3377.6	14953.7
	Creek	3631.5	-118.5	50988.4	5964.4	51107.0
	Forest Site 1	1614.2	-793.0	5726.6	1863.1	6519.6
	Forest Site 2	-649.7	-31832.8	87.3	3373.5	31920.0

Table 4 Mean, minimum, and maximum values, as well as standard deviation (SD) and interquartile range (IQR) of percent change for N_2O fluxes during the experiment (Phases I to V) for each soil.

		% Change N_2O				
		Mean	Minimum	Maximum	SD	IQR
All Phases	Wetland	54.5	-828.2	1749.8	384.7	2578.0
	Creek	58.8	-174.3	675.1	180.2	849.5
	Forest Site 1	3639.6	-113.2	55024.3	8799.2	55137.4
	Forest Site 2	-13699.9	-224510.8	2687.7	39313.5	227198.5
Phase I	Wetland	-15.1	-148.4	141.8	67.7	290.2
	Creek	99.4	-49.0	287.7	96.4	336.7
	Forest Site 1	-57.3	-113.2	51.5	43.8	164.7
	Forest Site 2	817.7	-1012.9	2687.7	963.4	3700.6
Phase II	Wetland	-38.1	-238.8	211.3	88.0	450.2
	Creek	-49.2	-150.6	257.3	101.1	407.9
	Forest Site 1	17789.1	-82.9	55024.3	13052.8	55107.2
	Forest Site 2	-61398.7	-224510.8	2066.9	68849.2	226577.7
Phase III	Wetland	347.7	-489.1	1749.8	521.8	2238.8
	Creek	101.7	-123.5	675.1	222.1	798.7
	Forest Site 1	2205.8	-59.4	19955.0	5279.2	20014.4
	Forest Site 2	-11184.3	-115411.1	394.5	30059.6	115805.6
Phase IV	Wetland	-245.1	-828.2	713.0	345.7	1541.2
	Creek	171.0	-101.4	637.7	268.0	739.1
	Forest Site 1	14.9	-38.8	168.4	35.6	207.2
	Forest Site 2	160.8	5.2	308.4	80.9	303.2
Phase V	Wetland	-91.1	-175.7	-2.5	39.2	173.2
	Creek	25.1	-174.3	206.8	94.5	381.2
	Forest Site 1	-18.4	-63.8	192.2	73.4	256.0
	Forest Site 2	-68.6	-99.6	242.7	65.5	342.4

Table 5 The percentages each soil (Wetland, Creek, Forest Site 1, Forest Site 2) contributed to the global warming potential (GWP) over the entire experiment for different combinations of greenhouse gases (CO_2, CH_4, and N_2O), illustrating the importance of measuring multiple greenhouse gases for 100 year and 20 year global warming potential (GWP) scenarios.

100 Year GWP	Wetland	Creek	Forest Site 1	Forest Site 2
CO_2	16.7%	33.6%	24.6%	25.1%
CH_4	78.8%	21.2%	1.9%	-2.0%
N_2O	0.8%	2.2%	41.0%	56.1%
CO_2 and CH_4	25.2%	32.0%	21.5%	21.4%
CO_2 and N_2O	1.7%	4.1%	40.0%	54.2%
CO_2, CH_4, and N_2O	2.5%	4.2%	39.7%	53.7%
20 Year GWP	Wetland	Creek	Forest Site 1	Forest Site 2
CO_2	16.7%	33.6%	24.6%	25.1%
CH_4	52.4%	42.9%	6.1%	-1.3%
N_2O	0.4%	7.6%	27.3%	64.7%
CO_2 and CH_4	20.0%	34.5%	22.9%	22.7%
CO_2 and N_2O	13.9%	29.2%	25.1%	31.8%
CO_2, CH_4, and N_2O	16.9%	30.3%	23.6%	29.2%

FIGURES

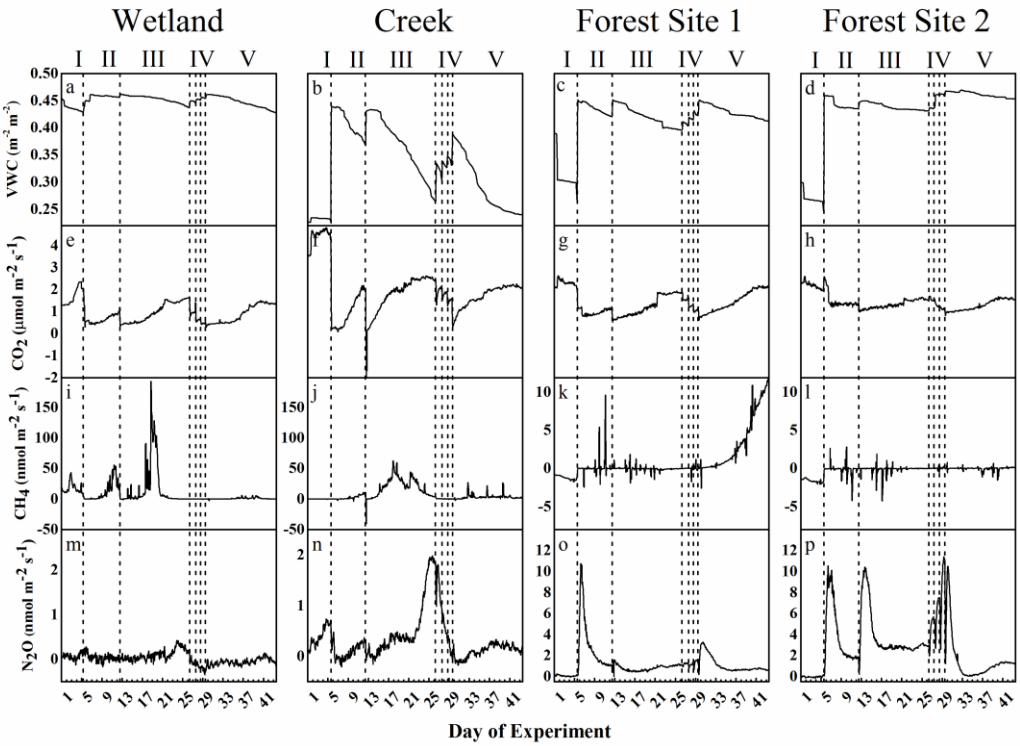

Figure 1 Time series of hourly data of GHGs (CO_2 CH_4, and N_2O) and volumetric water content (VWC) for Wetland (a, e, i, m) Creek (b, f, j, n), Forest Site 1 (c, g, k, o), and Forest Site 2 (d, h, l, p) soils. Vertical dashed lines represent the application of each water pulse. Roman numerals I-V denote Phases of the experiment.

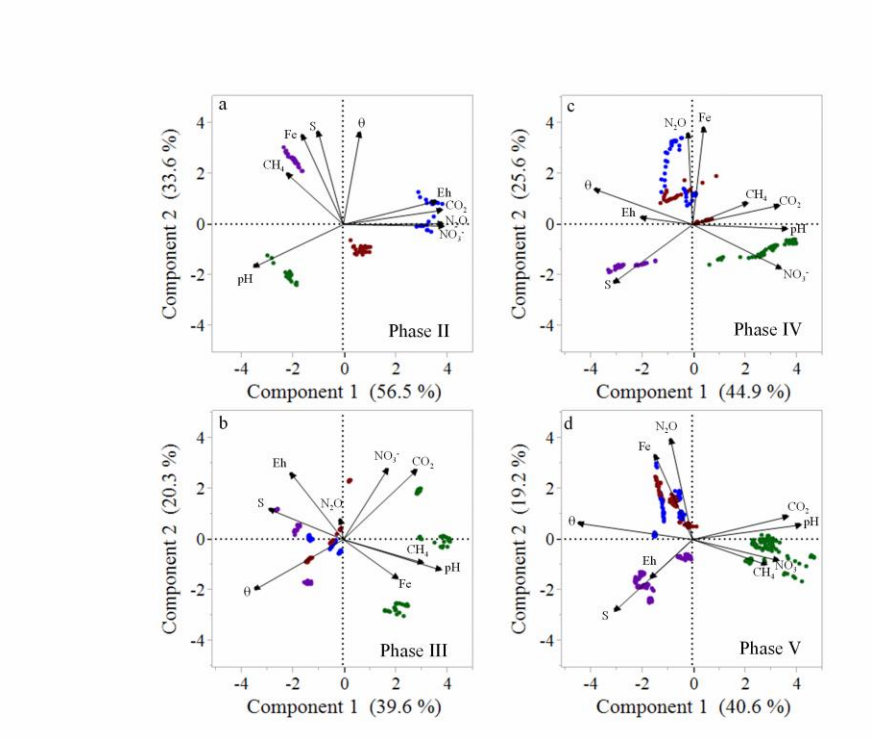

Figure 2 Principal Component Analysis (PCA) including fluxes of GHGs (CO_2 CH_4, and N_2O), measurements of porewater chemistry (Eh, pH, Fe, S, NO_3^-), and volumetric water content (θ) for all soils during Phases II, III, IV, and V (a, b, c, and d). Soils are represented by colored points: Purple represents the Wetland, Green represents the Creek, Red represents Forest Site 1, and Blue represents Forest Site 2.

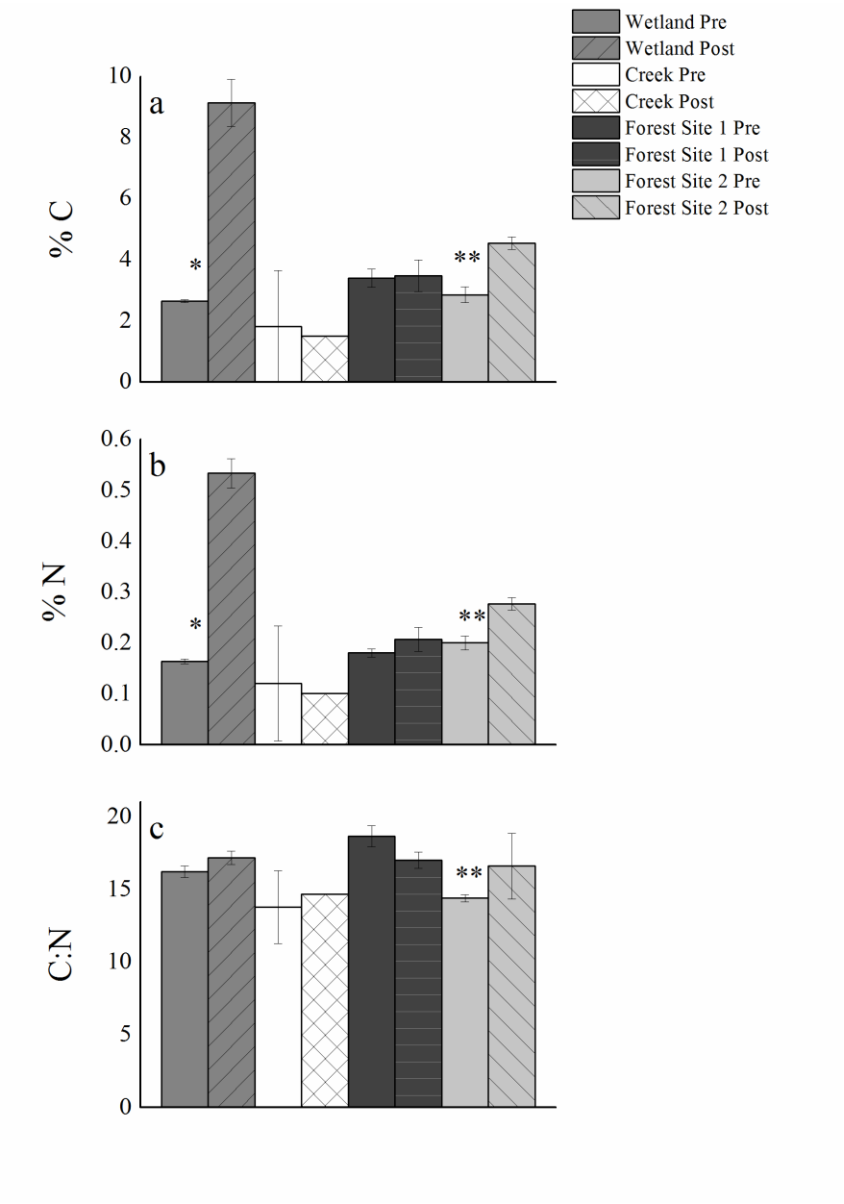

Figure 3 Means of percent C (a), percent N (b), and C:N ratio (c), for all soil locations before and after the re-wetting experiment. Significant differences between pre and post experimental conditions for C and N were found in the Wetland (**, $p<0.001$) and Forest Site 2 (*, $p<0.05$) soils. Forest Site 2 also showed a significant difference for pre and post experimental C:N (**, $p<0.001$) . Error bars display one standard deviation from the mean. Solid bars indicate pre-experimental values. Patterned bars indicate post-experimental values.

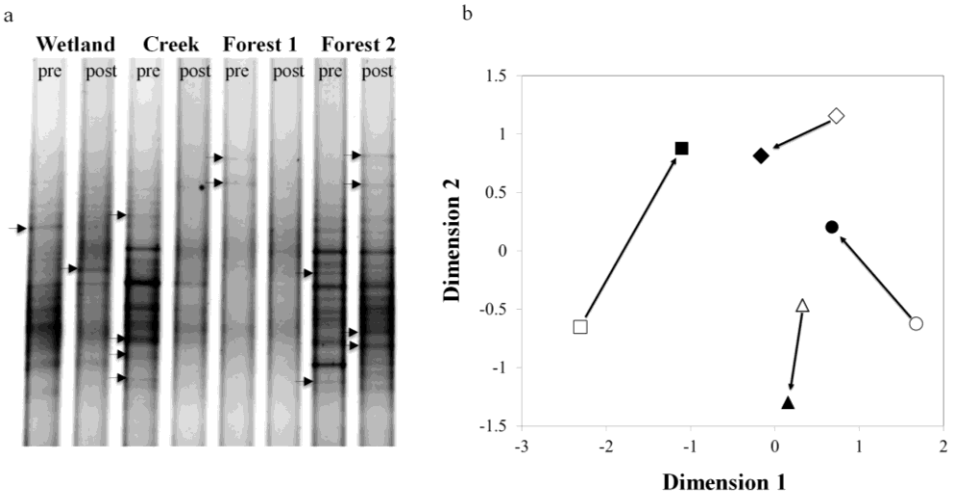

Figure 4 DGGE gel (a) showing differences in bands (arrows) for pre and post experiment conditions, labeled by soil (Wetland, Creek, Forest Site 1, and Forest Site 2), and Non-metric Multidimensional Scaling (NMDS) plots of bacterial community structure based on presence/absence of DGGE banding patterns (b). Shifts in Microbial Community Structure between the beginning (open markers) and end (closed markers) of the experiment were shown from samples of Wetland (triangles), Creek (diamonds), Forest Site 1 (squares), and Forest Site 2 (circles) soils.

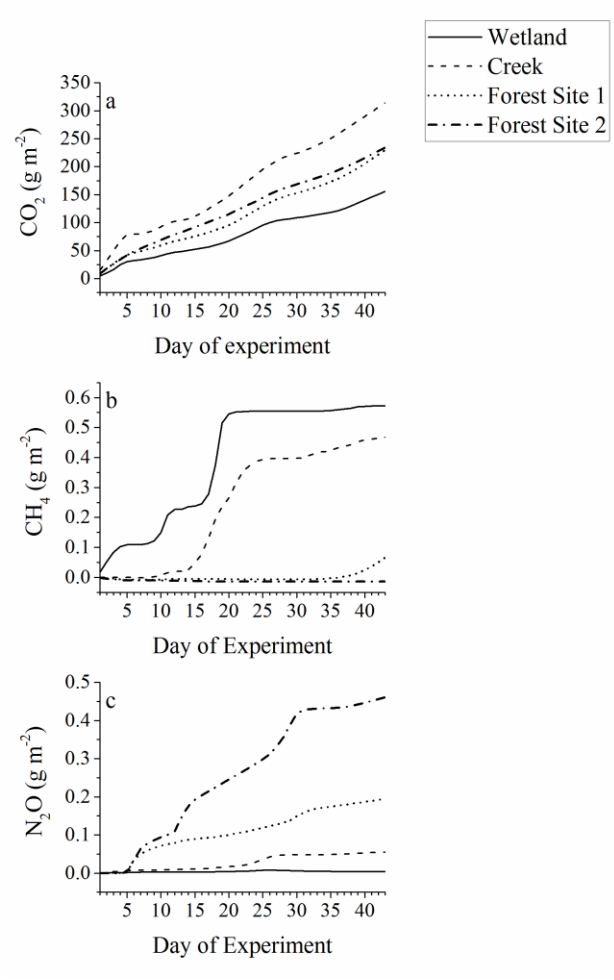

Figure 5 Cumulative mean daily concentrations of CO_2 (a), CH_4 (b), and N_2O, given as g m^{-2}, for the Wetland (solid line), Creek (dashed line), Forest Site 1 (dotted line) and Forest Site 2 (dash-dotted line) soils. The cumulative amounts are total summations of each gas, for each soil, generated during the experiment. The cumulative amounts of each greenhouse gas, generated over the whole of the experiment, can then be converted into CO_2 equivalences ($CO_{2\text{-eq}}$), which illustrates the global warming potentials as $CO_{2\text{-eq}}$ for each soil.

Chapter 3

FUTURE APPLICATIONS AND POLICY IMPLICATIONS

This experiment provided unique insight to GHG flux dynamics for CO_2, CH_4, and N_2O from soils which were subjected to extreme inundated conditions through repeated water pulses. High temporal frequency measurements successfully monitored these rapidly changing conditions in soil moisture, and GHG fluxes, and discrete measurements of porewater and soils for chemical and microbial analysis. Future experiments would also benefit from coupling near-continuous, high temporal frequency measurements with soil moisture and temperature, and should also include continuous measurements of Eh. Furthermore, such datasets could be useful for modeling applications, which would be able to simulate potential changes to GHG fluxes as a result of extreme hydrologic events.

The impacts of extreme events are often threshold based, and highly nonlinear (Frank et al. 2015). An extreme weather event is defined as such if it breaches a threshold of observed values for a particular reference period of time. The water pulses administered during the experiment led to abnormally wet conditions within soils, although they did not replicate the amount of rainfall from a specific storm event. Although historic measurements could have been used to apply an equivalent amount of water deposited during large storms, such as hurricane Irene, it was decided that to avoid overflow of water from mesocosms, and thus loss of water, dissolved solutes, and soil, that we reduced the size of the pulses, while also creating and maintaining the extreme wet conditions.

Soil sampling locations were selected to explore the potential for change among different soils, and account for the wide range of natural variation present within our study site. The requirement for a continuous power supply for these instruments, the limitations of extension cable lengths which reach 16m, and the high cost of instrumentation presented a challenge for replication of measurements in our experimental design. Furthermore, this multiplexed system can only activate measurements for one chamber at a time. Thus, the experiment focused on changes at high temporal frequency, rather than a traditional experimentalist approach involving high spatial replication. We also utilized 20cm diameter soil collars for our mesocosms, in favor of smaller cores, and increasing the number of automated chambers used during the experiment.

We were also unable to account for the natural hydrologic connectivity of soils along the topographic gradient from which we sampled. Other experiments have prevented the lateral flow of water and transport of solutes while exploring the influence of water on GHG fluxes from soils (Xu and Luo 2012), and although influence of lateral transport of solutes is important and occurs naturally (Creed and Beall 2009), it was unrealistic for us to do so in this experiment. This was due to the necessary arrangement of mesocosms in the laboratory and the manner in which our instruments measure. Each chamber must form a seal over the PVC collars to properly measure gas concentrations and calculate gas flux, without which accurate automated high temporal frequency chamber measurements are rendered impossible. Creating an artificial gradient would have required a large removal of soils from the sampling location, which would have been disruptive to both the watershed and the soils, and would not have allowed us to maintain intact mesocosms. It would also increase the

risk of an improper placement of soil collars, leading to lateral diffusion of GHGs, and an underestimation of GHG fluxes (Görres et al. 2015).

Policy solutions and management strategies to mitigate the impacts of extreme events on GHG fluxes from soils should be proactive, pragmatic, and equitable. The relationship between societal interactions with an ecosystem requires communication between scientists and policymakers. Additionally, any policy decisions made with regards to attempts to mitigate GHG fluxes from soils should ensure that they meet the needs of, recognize, and include the knowledge and voices of vulnerable populations (e.g.: resource-based communities, and indigenous peoples) (Lynn et al. 2011). In light of the unprecedented changes in magnitude of GHG fluxes observed in this experiment, it is possible that extreme events could inhibit CO_2 fluxes, but promote fluxes of CH_4 and N_2O which due to the unique GWP of each gas (IPCC 2007) could exacerbate global warming. The "Fraction Attributable Risk" or FAR method describes the proportion of the probability of an extreme event occurring due to increased concentrations of atmospheric GHGs, and has also been used in analysis of northern-hemisphere rainfall (McGee et al. 2013). Perhaps using this as a metric for exploring feedback of soil GHG flux responses to extreme events addition to GWP would be useful in future studies.

REFERENCES

Aber J, Stange F, Butterbach-bahl K, et al (2000) A process-oriented model of N2O and NO emissions from forest soils: 1. Model development. J Geophys Res 105:4369–4384.

Barron-Gafford G a., Scott RL, Jenerette GD, Huxman TE (2011) The relative controls of temperature, soil moisture, and plant functional group on soil CO2 efflux at diel, seasonal, and annual scales. J Geophys Res Biogeosciences 116:G01023. doi: 10.1029/2010JG001442

Bodelier PL., Laanbroek HJ (2004) Nitrogen as a regulatory factor of methane oxidation in soils and sediments. FEMS Microbiol Ecol 47:265–277. doi: 10.1016/S0168-6496(03)00304-0

Borken W, Matzner E (2009) Reappraisal of drying and wetting effects on C and N mineralization and fluxes in soils. Glob Chang Biol 15:808–824. doi: 10.1111/j.1365-2486.2008.01681.x

Chapin FSI, Matson PA, Vitousek PM (2011) Principles of Terrestrial Ecosystem Ecology, Second. Springer New York, New York, NY

Christiansen JR, Gundersen P, Frederiksen P, Vesterdal L (2012) Influence of hydromorphic soil conditions on greenhouse gas emissions and soil carbon stocks in a Danish temperate forest. For Ecol Manage 284:185–195. doi: 10.1016/j.foreco.2012.07.048

Cirmo CP, McDonnell JJ (1997) Linking the hydrologic and biogeochemical controls of nitrogen transport in near-stream zones of temperate-forested catchments: A review. J Hydrol 199:88–120. doi: 10.1016/S0022-1694(96)03286-6

Cisneros-Dozal LM, Trumbore SE, Hanson PJ (2007) Effect of moisture on leaf litter decomposition and its contribution to soil respiration in a temperate forest. J Geophys Res 112:G01013. doi: 10.1029/2006JG000197

Creed IF, Beall FD (2009) Distributed topographic indicators for predicting nitrogen export from headwater catchments. Water Resour Res. doi: 10.1029/2008WR007285

Dai Z, Trettin CC, Li C (2012) Effect of Assessment Scale on Spatial and Temporal Variations in CH 4 , CO 2 , and N 2 O Fluxes in a Forested Wetland. 253–265. doi: 10.1007/s11270-011-0855-0

Dalal RC, Allen DE, Livesley SJ, Richards G (2008) Magnitude and biophysical regulators of methane emission and consumption in the Australian agricultural, forest, and submerged landscapes: A review.

Davidson E a, Belk E, Boone RD (1998) Soil water content and temperature as independent or confounded factors controlling soil respiration in a temperate mixed hardwood forest. Glob Chang Biol 4:217–227. doi: 10.1046/j.1365-2486.1998.00128.x

Davidson EA, Savage KE, Finzi AC (2014) A big-microsite framework for soil carbon modeling. Glob Chang Biol 20:3610–3620. doi: 10.1111/gcb.12718

Dhillon GS, Inamdar S (2013) Extreme storms and changes in particulate and dissolved organic carbon in runoff: Entering uncharted waters? Geophys Res Lett 40:1322–1327. doi: 10.1002/grl.50306

Enanga EM, Creed IF, Casson NJ, Beall FD (2015) Summer storms trigger soil N2O efflux episodes in forested catchments. J Geophys Res Biogeosciences 1–14. doi: 10.1002/2015JG003027.Received

Erickson HE, Perakis SS (2014) Soil fluxes of methane, nitrous oxide, and nitric oxide from aggrading forests in coastal Oregon. Soil Biol Biochem 76:268–277. doi: 10.1016/j.soilbio.2014.05.024

Essington ME (2004) Soil and Water Chemistry An Integrative Approach. CRC Press, Boca Raton, Florida

Fierer N, Jackson RB (1998) The diversity and biogeography of soil bacterial communities. Pnas 103:626–631. doi: 10.1073/pnas.0507535103|ISSN 0027-8424

Fierer N, Schimel JP (2002) Effects of drying–rewetting frequency on soil carbon and nitrogen transformations. Soil Biol Biochem 34:777–787. doi: 10.1016/S0038-0717(02)00007-X

Fierer N, Schimel JP (2003) A Proposed Mechanism for the Pulse in Carbon Dioxide Production Commonly Observed Following the Rapid Rewetting of a Dry Soil. Soil Sci Soc Am J 67:798. doi: 10.2136/sssaj2003.0798

Frank D, Reichstein M, Bahn M, et al (2015) Effects of climate extremes on the terrestrial carbon cycle: Concepts, processes and potential future impacts. Glob Chang Biol 21:2861–2880. doi: 10.1111/gcb.12916

Görres C-M, Kammann C, Ceulemans R (2015) Automation of soil flux chamber

measurements: potentials and pitfalls. Biogeosciences Discuss 12:14693–14738. doi: 10.5194/bgd-12-14693-2015

Grybos M, Davranche M, Gruau G, et al (2009) Increasing pH drives organic matter solubilization from wetland soils under reducing conditions. Geoderma 154:13–19. doi: 10.1016/j.geoderma.2009.09.001

Hall S, McDowell W, Silver W (2013) When wet gets wetter: decoupling of moisture, redox biogeochemistry, and greenhouse gas fluxes in a humid tropical forest soil. Ecosystems 16:576–589. doi: 10.1007/s10021-012-9631-2

Hartmann DL, Tank AMGK, Rusticucci M (2013) IPCC Fifth Assessment Report, Climatie Change 2013: The Physical Science Basis.

Haugwitz MS, Bergmark L, Priemé A, et al (2014) Soil microorganisms respond to five years of climate change manipulations and elevated atmospheric CO2 in a temperate heath ecosystem. Plant Soil 374:211–222. doi: 10.1007/s11104-013-1855-1

IPCC (2013) Climate Change 2013: The Physical Science Basis. Contribution of Working Group I to the Fifth Assessment Report of the Intergovernmental Panel on Climate Change. Cambridge University Press, Cambridge and New York

IPCC (2007) Climate change 2007 : the physical science basis : contribution of Working Group I to the Fourth Assessment Report of the Intergovernmental Panel on Climate Change. Cambridge ; New York : Cambridge University Press, 2007.

Jenkins S, Gibson N (2002) High-throughput SNP genotyping. Comp Funct Genomics 3:57–66. doi: 10.1002/cfg.130

Kan J, Wang K, Chen F (2006) Temporal variation and detection limit of an estuarine bacterioplankton community analyzed by denaturing gradient gel electrophoresis (DGGE). Aquat Microb Ecol 42:7–18. doi: 10.3354/ame042007

Kim D-G, Vargas R, Bond-Lamberty B, Turetsky MR (2012) Effects of soil rewetting and thawing on soil gas fluxes: a review of current literature and suggestions for future research. Biogeosciences 9:2459–2483. doi: 10.5194/bg-9-2459-2012

Kim SY, Veraart AJ, Meima-Franke M, Bodelier PLE (2015) Combined effects of carbon, nitrogen and phosphorus on CH4 production and denitrification in wetland sediments. Geoderma 259-260:354–361. doi: 10.1016/j.geoderma.2015.03.015

Knapp AK, Beier C, Briske DD, et al (2008) Consequences of More Extreme Precipitation Regimes for Terrestrial Ecosystems. Bioscience 58:811. doi: 10.1641/B580908

Le Mer J, Roger P (2001) Production, oxidation, emission and consumption of methane by soils: a review.

Leon E, Vargas R, Bullock S, et al (2014) Hot spots, hot moments, and spatio-temporal controls on soil CO2 efflux in a water-limited ecosystem. Soil Biol Biochem 77:12–21. doi: 10.1016/j.soilbio.2014.05.029

Levia DF, Carlyle-Moses D, Tanaka T (2011) Forest hydrology and biogeochemistry [Electronic book] : synthesis of past research and future directions. Springer Science+Business Media

Lynn K, MacKendrick K, Donoghue EM (2011) Social Vulnerability and Climate Change: Synthesis of Literature.

Manzoni S, Porporato A (2009) Soil carbon and nitrogen mineralization: Theory and models across scales. Soil Biol Biochem 41:1355–1379. doi: 10.1016/j.soilbio.2009.02.031

McDaniel MD, Kaye JP, Kaye MW (2014) Do ???hot moments??? become hotter under climate change? Soil nitrogen dynamics from a climate manipulation experiment in a post-harvest forest. Biogeochemistry 121:339–354. doi: 10.1007/s10533-014-0001-3

McGee J, Phelan L, Wenta J (2013) Writing the Fine Print: Developing Regional Insurance for Climate Change Adaptation in the Pacific. Melb J Int Law 15:1–29.

McNicol G, Silver WL (2014) Separate effects of flooding and anaerobiosis on soil greenhouse gas emissions and redox sensitive biogeochemistry. J Geophys Res Biogeosciences 119:557–566. doi: 10.1002/2013JG002433.Received

McNicol G, Silver WL (2015) Non-linear response of carbon dioxide and methane emissions to oxygen availability in a drained histosol. Biogeochemistry 123:299–306. doi: 10.1007/s10533-015-0075-6

Muhr J, Goldberg S, Borken W, Gebauer G (2008) Repeated drying–rewetting cycles and their effects on the emission of CO2, N2O, NO, and CH4 in a forest soil. J Plant Nutr Soil Sci 171:719–728. doi: 10.1002/jpln.200700302

Muyzer G, De Waal EC, Uitterlinden AG (1993) Profiling of complex microbial populations by denaturing gradient gel electrophoresis analysis of polymerase

chain reaction-amplified genes coding for 16S rRNA. Appl Environ Microbiol 59:695–700.

Myhre G, Shindell D, Bréon F-M, et al (2013) 2013: Anthropogenic and Natural Radiative Forcing. In: Stocker TF, Qin D, Plattner G-K, et al. (eds) Climate Change 2013: The Physical Science Basis. Contribution of Working Group I to the Fifth Assessment Report of the Intergovernmental Panel on Climate Change. Cambridge University Press, Cambridge, United Kingdom and New York, NY, USA, pp 659–740

Pachauri RK, Allen MR, Barros VR, et al (2014) IPCC, 2014: CLIMATE CHANGE 2014 Synthesis Report Summary for Policymakers.

Pacific VJ, McGlynn BL, Riveros-Iregui DA, et al (2009) Differential soil respiration responses to changing hydrologic regimes. Water Resour Res 45:6–11. doi: 10.1029/2009WR007721

Paul S, Kusel K, Alewell C (2006) Reduction processes in forest wetlands: Tracking down heterogeneity of source/sink functions with a combination of methods. Soil Biol Biochem 38:1028–1039. doi: 10.1016/j.soilbio.2005.09.001

Pearson AJ, Pizzuto JE, Vargas R (2016) Influence of run of river dams on floodplain sediments and carbon dynamics. Geoderma 272:51–63. doi: 10.1016/j.geoderma.2016.02.029

Pester M, Knorr KH, Friedrich MW, et al (2012) Sulfate-reducing microorganisms in wetlands - fameless actors in carbon cycling and climate change. Front Microbiol 3:1–19. doi: 10.3389/fmicb.2012.00072

Pilegaard K, Skiba U, Ambus P, et al (2006) Factors controlling regional differences in forest soil emission of nitrogen oxides (NO and N 2 O). Biogeosciences 3:651–661.

Riveros-Iregui DA, McGlynn BL (2009) Landscape structure control on soil CO2 efflux variability in complex terrain: Scaling from point observations to watershed scale fluxes. J Geophys Res Biogeosciences. doi: 10.1029/2008JG000885

Sagan D, Margulis L (1993) Garden of Microbial Delights A Practical Guide To The Subvisible World, 1993rd edn. Kendall Hunt Publsihing Company

Savage K, Phillips R, Davidson E (2014) High temporal frequency measurements of greenhouse gas emissions from soils. Biogeosciences 11:2709–2720. doi: 10.5194/bg-11-2709-2014

Savage KE, Davidson E a. (2003) A comparison of manual and automated systems for soil CO2 flux measurements: Trade-offs between spatial and temporal resolution. J Exp Bot 54:891–899. doi: 10.1093/jxb/erg121

Schimel J, Balser TC, Wallenstein M (2007) Microbial stress-response physiology and its implications for ecosystem function. Ecology 88:1386–1394. doi: 10.1890/06-0219

Schlesinger W, Andrews J (2000) Soil respiration and the global carbon cycle. Biogeochemistry 48:7–20. doi: 10.1023/A:1006247623877

Seneviratne SI, Corti T, Davin EL, et al (2010) Investigating soil moisture–climate interactions in a changing climate: A review. Earth-Science Rev 99:125–161. doi: 10.1016/j.earscirev.2010.02.004

Serrano-Silva N, Sarria-Guzmán Y, Dendooven L, Luna-Guido M (2014) Methanogenesis and Methanotrophy in Soil: A Review. Pedosphere 24:291–307. doi: 10.1016/S1002-0160(14)60016-3

Seyfferth AL, Fendorf S (2012) Silicate mineral impacts on the uptake and storage of arsenic and plant nutrients in rice (Oryza sativa L.). Environ Sci Technol 46:13176–13183. doi: 10.1021/es3025337

Smith K a., Ball T, Conen F, et al (2003) Exchange of greenhousegases between soil and atmosphere: interactions of soil physical factors and biological processes. Eur J Soil Sci 54:779–791. doi: 10.1046/j.1365-2389.2003.00567.x

Steduto P, Çetinkökü Ö, Albrizio R, Kanber R (2002) Automated closed-system canopy-chamber for continuous field-crop monitoring of CO2 and H2O fluxes. Agric For Meteorol 111:171–186. doi: 10.1016/S0168-1923(02)00023-0

Sutherland WJ, Freckleton RP, Godfray HCJ, et al (2013) Identification of 100 fundamental ecological questions. J Ecol 101:58–67. doi: 10.1111/1365-2745.12025

Tian H, Lu C, Ciais P, et al (2016) The terrestrial biosphere as a net source of greenhouse gases to the atmosphere. Nature 531:225–228. doi: 10.1038/nature16946

Vargas R (2012) How a hurricane disturbance influences extreme CO 2 fluxes and variance in a tropical forest. Environ Res Lett 7:035704. doi: 10.1088/1748-9326/7/3/035704

Vargas R, Carbone MS, Reichstein M, Baldocchi DD (2011) Frontiers and challenges

in soil respiration research: From measurements to model-data integration. Biogeochemistry 102:1–13. doi: 10.1007/s10533-010-9462-1

Vargas R, Collins SL, Thomey ML, et al (2012) Precipitation variability and fire influence the temporal dynamics of soil CO 2 efflux in an arid grassland. Glob Chang Biol 18:1401–1411. doi: 10.1111/j.1365-2486.2011.02628.x

Wang X, Liu L, Piao S, et al (2014) Soil respiration under climate warming: differential response of heterotrophic and autotrophic respiration. Glob Chang Biol 20:3229–37. doi: 10.1111/gcb.12620

Wu L, Rees RM, Tarsitano D, et al (2015) Simulation of nitrous oxide emissions at field scale using the SPACSYS model. Sci Total Environ 530-531:76–86. doi: 10.1016/j.scitotenv.2015.05.064

Xu X, Luo X (2012) Effect of wetting intensity on soil GHG fluxes and microbial biomass under a temperate forest floor during dry season. Geoderma 170:118–126. doi: 10.1016/j.geoderma.2011.11.016

Zhuang Q, Zhu X, He Y, et al (2004) In fl uence of changes in wetland inundation extent on net fl uxes of carbon dioxide and methane in northern high latitudes from 1993 to 2004. Environ Res Lett 10:95009. doi: 10.1088/1748-9326/10/9/095009

Appendix

SUPPLEMENTARY MATERIALS

Supplementary material 1 – Examples of changing concentrations of CO_2 (a), CH_4 (b) and N_2O (c), in parts per million, from the Picarro G2508 during measurements. These concentrations were used to calculate gas fluxes for each greenhouse gas using equation 1.

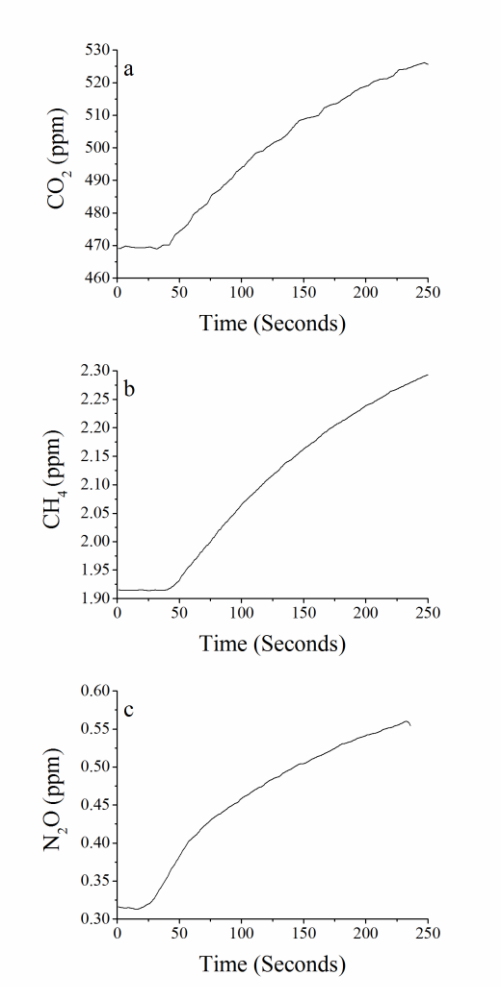

Supplementary material 2 – Percent change of CO_2 for each soil, by Phase. Wetland soil, phases I-V (a-e); Creek soil, phases I-V (f-j); Forest Site 1 soil, phases I-V (k-o); Forest Site 2 soil phases I-V (p-t).

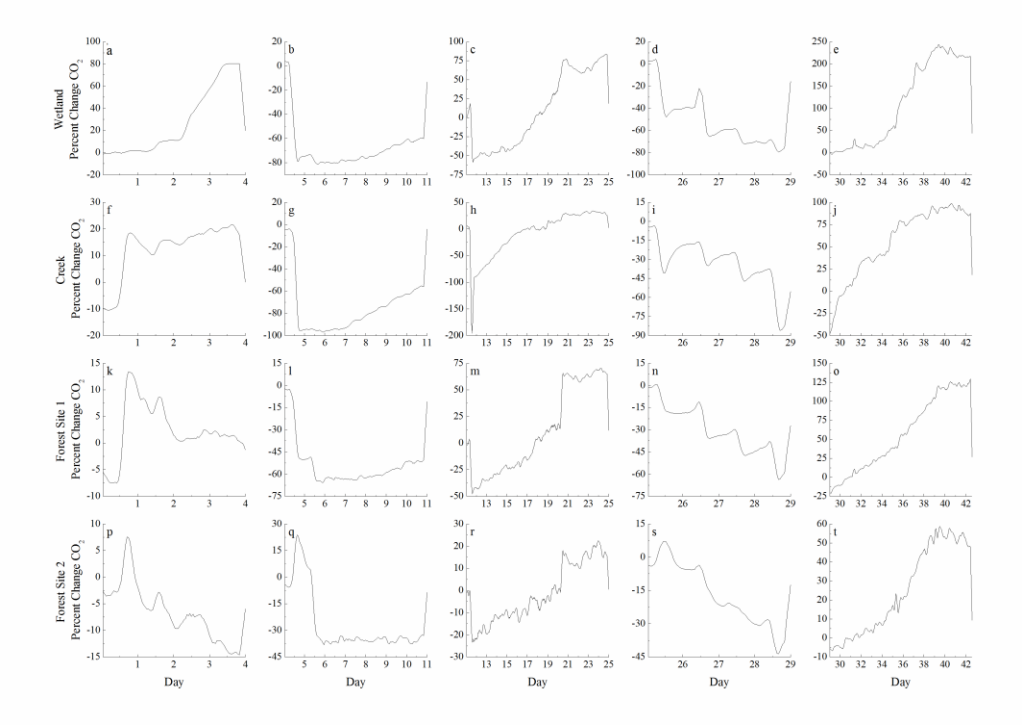

Supplementary material 3 – Percent change of CH_4 for each soil, by Phase. Wetland soil, Phases I-V (a-e); Creek soil, Phases I-V (f-j); Forest Site 1 soil, Phases I-V (k-o); Forest Site 2 soil Phases I-V (p-t).

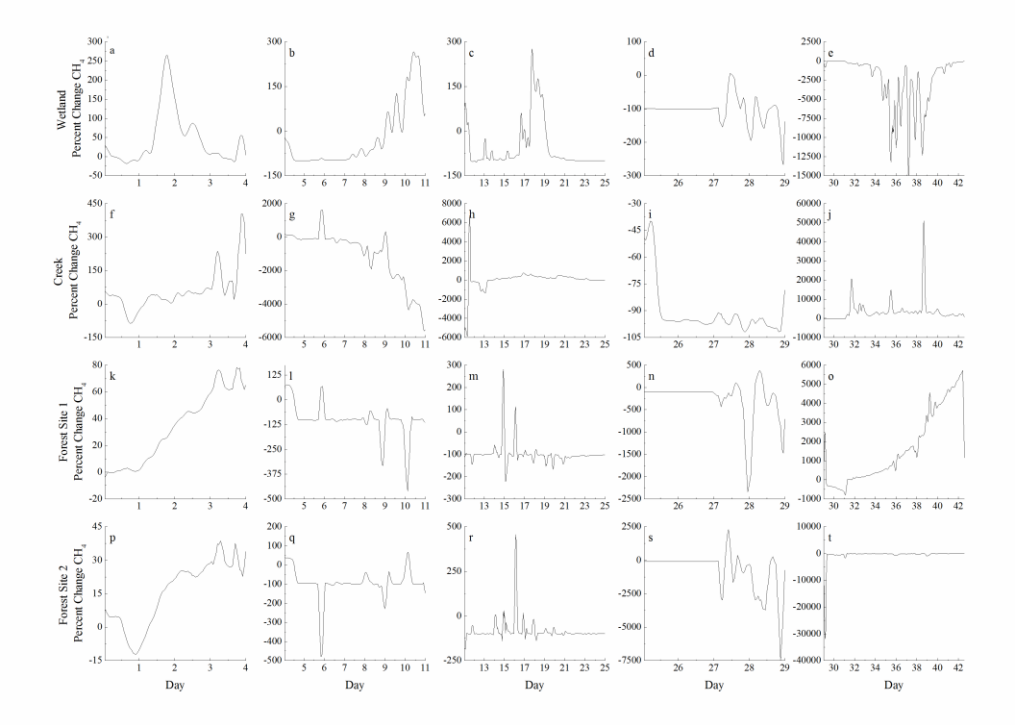

Supplementary material 4 – Percent change of N_2O for each soil, by Phase. Wetland soil, Phases I-V (a-e); Creek soil, Phases I-V (f-j); Forest Site 1 soil, Phases I-V (k-o); Forest Site 2 soil Phases I-V (p-t).

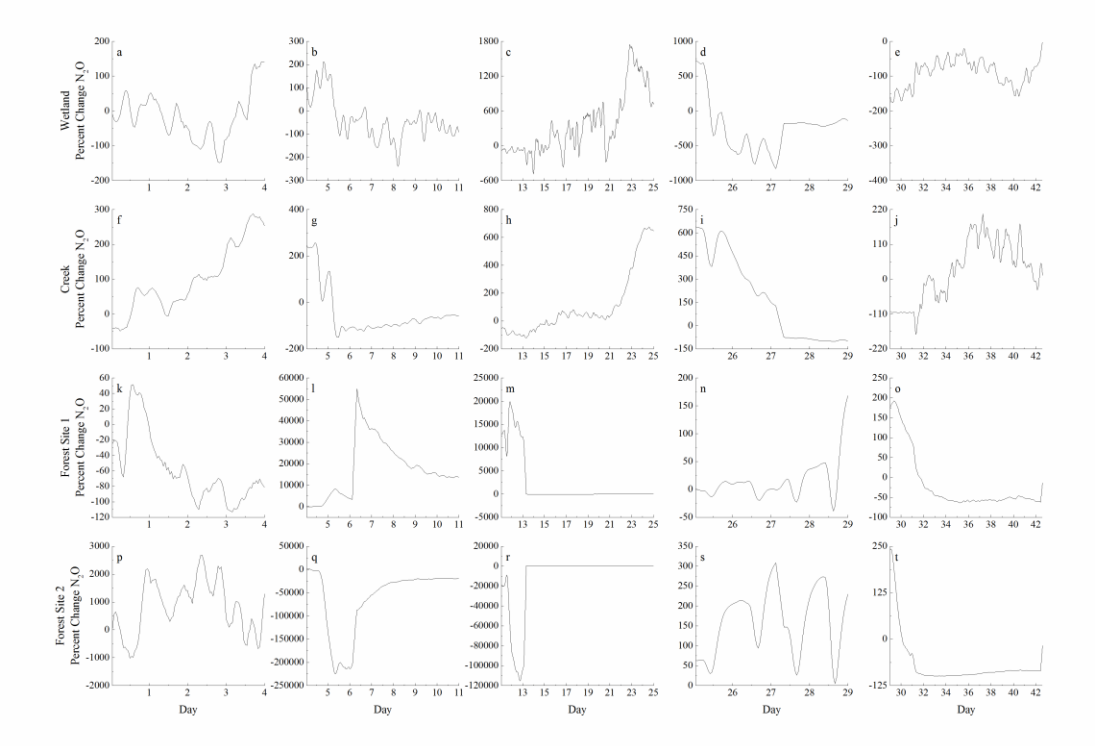

Supplementary material 5 – Relationships between greenhouse gases for each of the soils. Error bars represent one standard deviation. Mean gas fluxes for each Phase were calculated and used to generate the five points for each panel. Only one combination of greenhouse gases for the Wetland soil had a significant ($p<0.05$) linear relationship (c).

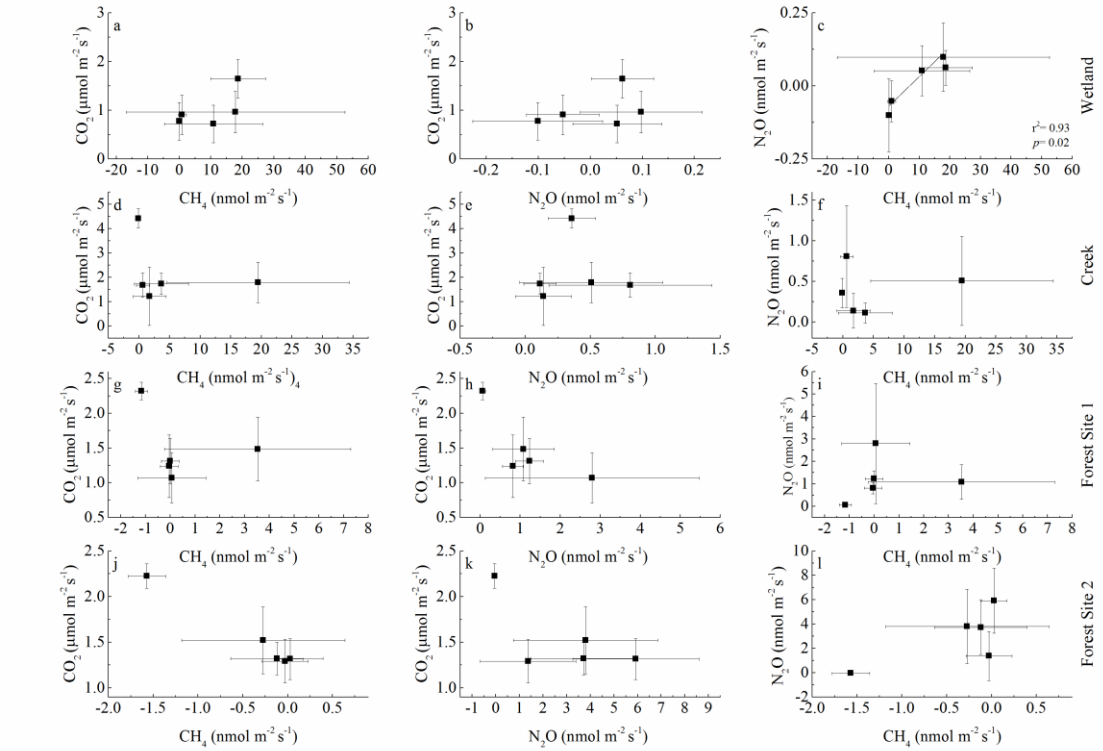

Supplementary material 6 – Relationships between greenhouse gas fluxes and different variables for porewater chemistry from the Wetland soil. Error bars represent one standard deviation. Mean values for Phases II-V were used, as porewater samples were not extracted in Phase I of the experiment. Only CO_2 and Sulfur showed a significant ($p<0.05$) linear relationship (j).

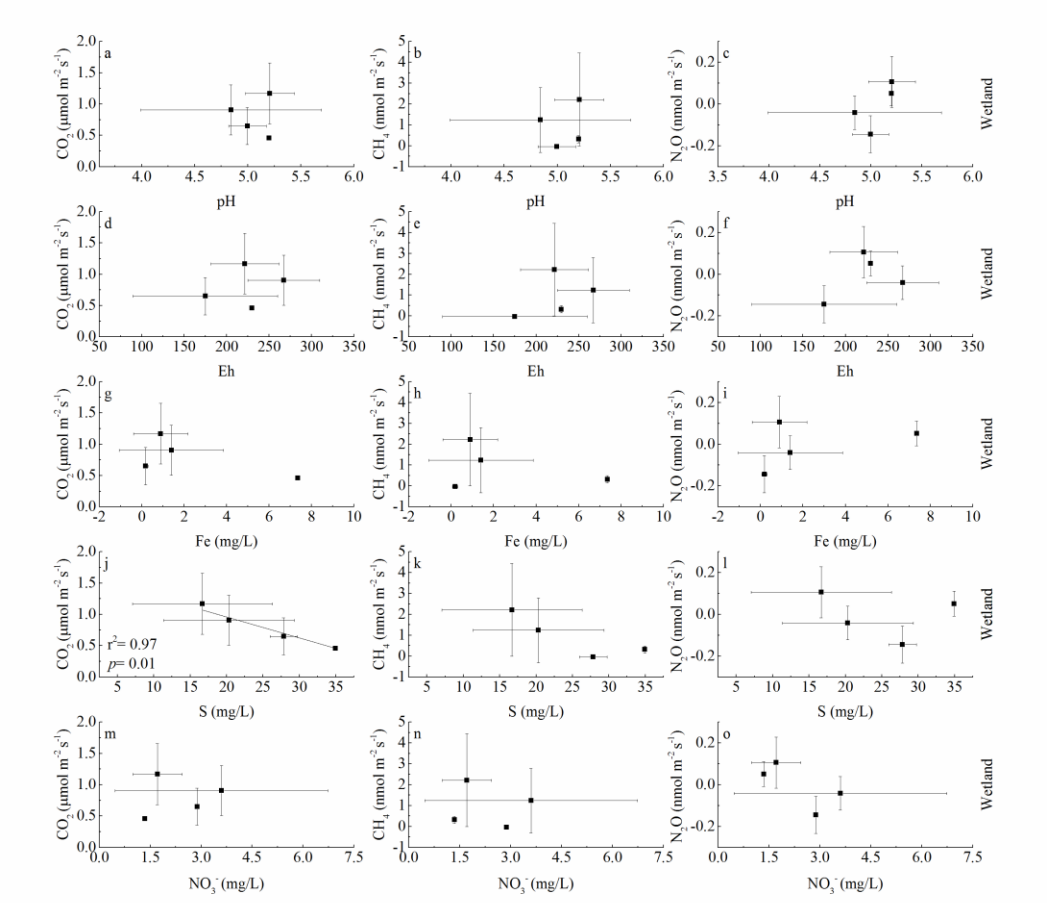

Supplementary material 7 – Relationships between greenhouse gas fluxes and different variables for porewater chemistry from the Creek soil. Error bars represent one standard deviation. Mean values for Phases II-V were used, as porewater samples were not extracted in Phase I of the experiment. Only CO_2 and Sulfur showed a significant ($p<0.05$) linear relationship (j).

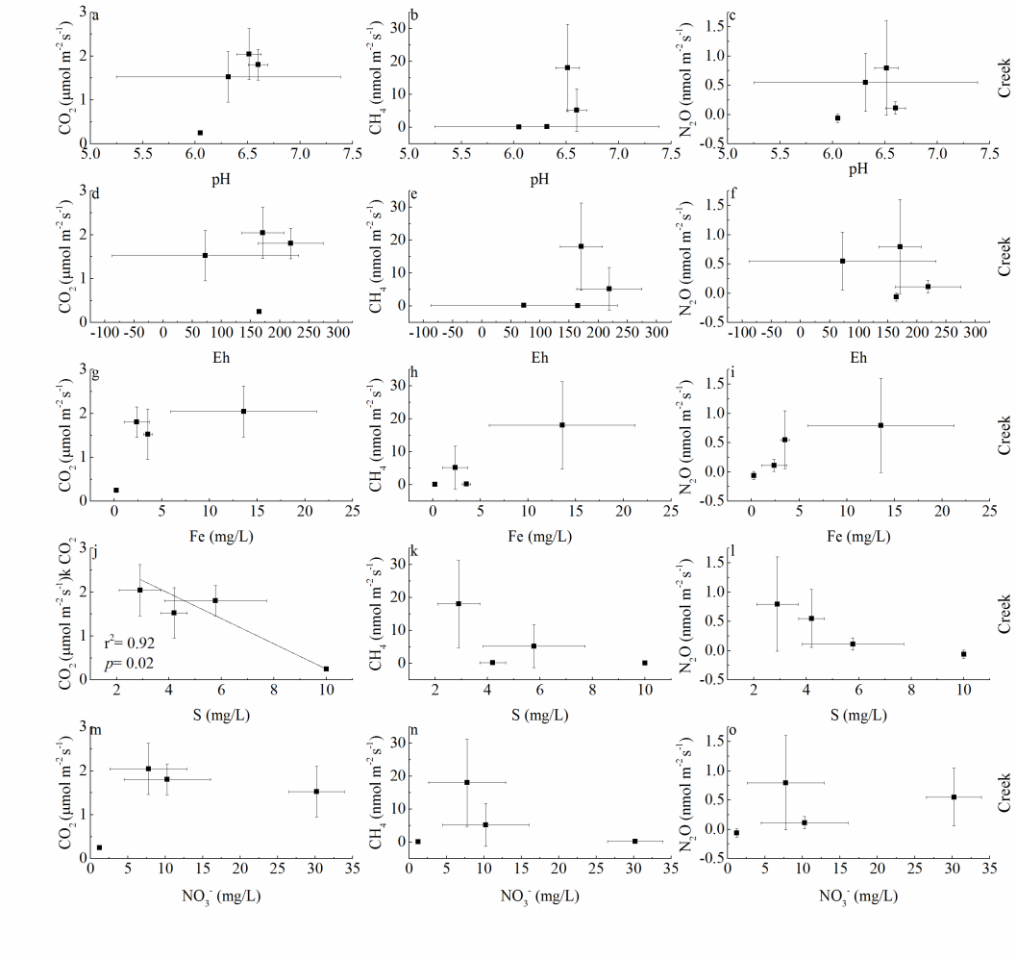

Supplementary material 8 – Relationships between greenhouse gas fluxes and different variables for porewater chemistry from the Forest Site 2 soil. Error bars represent one standard deviation. Mean values for Phases II-V were used, as porewater samples were not extracted in Phase I of the experiment. Only N_2O and Iron showed a significant ($p<0.05$) linear relationship (i).

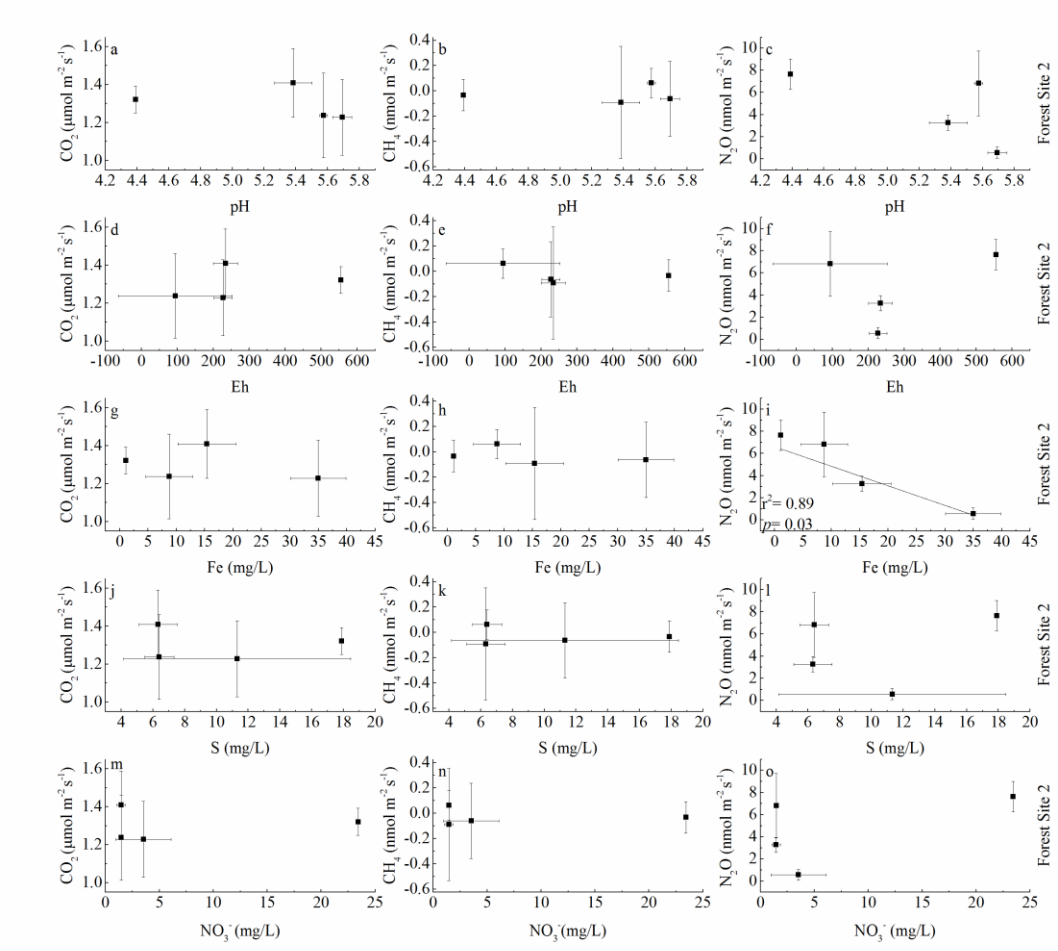

Supplementary material 9 – Global Warming Potential values as CO_2 equivalencies ($CO_{2\text{-eq}}$) of GHG fluxes in g m^{-2}, using 20 and 100 year Global Warming Potential values for each of the four soils (Wetland, Creek, Forest Site 1, and Forest Site 2) for the entire length of the experiment.

	CO_2 g m^{-2}	CH4 ($CO_{2\text{-eq}}$) g m^{-2}		N2O ($CO_{2\text{-eq}}$) g m^{-2}	
	20 and 100 Year GWP	20 Year GWP	100 Year GWP	20 Year GWP	100 Year GWP
Wetland	155.94	49.15	116.18	0.84	109.38
Creek	314.07	40.22	31.26	14.6	309.66
Forest Site 1	229.62	5.7	2.81	52.11	5917.68
Forest Site 2	233.88	-1.2	-2.9	123.69	8089.43

Supplementary material 10 – Loadings from principal component analysis including eigenvalues for Component 1 and Component 2, as well as the loadings for porewater chemistry (pH, Eh, Fe, S, and NO_3^-), greenhouse gas fluxes (CO_2, CH_4, and N_2O), and volumetric water content (θ).

Eigenvalues	Phase II		Phase III		Phase IV		Phase V	
	Eigenvalue	Percent	Eigenvalue	Percent	Eigenvalue	Percent	Eigenvalue	Percent
1	5.08	56.45	3.56	39.58	4.04	44.94	3.66	40.63
2	3.03	33.64	1.83	20.34	2.31	25.62	1.72	19.16
Loadings	Phase II		Phase III		Phase IV		Phase V	
	PC1	PC2	PC1	PC2	PC1	PC2	PC1	PC2
CO2	0.98	0.14	0.68	0.65	0.81	0.18	0.77	0.19
N2O	0.98	0.01	-0.03	0.18	-0.04	0.88	-0.18	0.82
CH4	-0.56	0.51	0.73	-0.22	0.51	0.20	0.59	-0.21
pH	-0.88	-0.42	0.90	-0.28	0.89	-0.04	0.87	0.12
Eh	0.92	0.24	-0.48	0.62	-0.48	0.07	-0.33	-0.31
NO3-	0.99	-0.01	0.41	0.66	0.83	-0.42	0.69	-0.17
Fe	-0.41	0.90	0.50	-0.36	0.10	0.93	-0.30	0.69
S	-0.25	0.93	-0.68	0.28	-0.75	-0.56	-0.63	-0.58
θ	0.17	0.92	-0.81	-0.47	-0.92	0.34	-0.92	0.13

Supplementary material 11 – Porewater concentrations for Nitrate (NO_3^-) from samples drawn from the Wetland (solid line, open squares), Creek (dotted line, open circles), Forest Site 1 (short dashed line, open upward triangles), and Forest Site 2 (long dashed line, open downward triangles) soils.